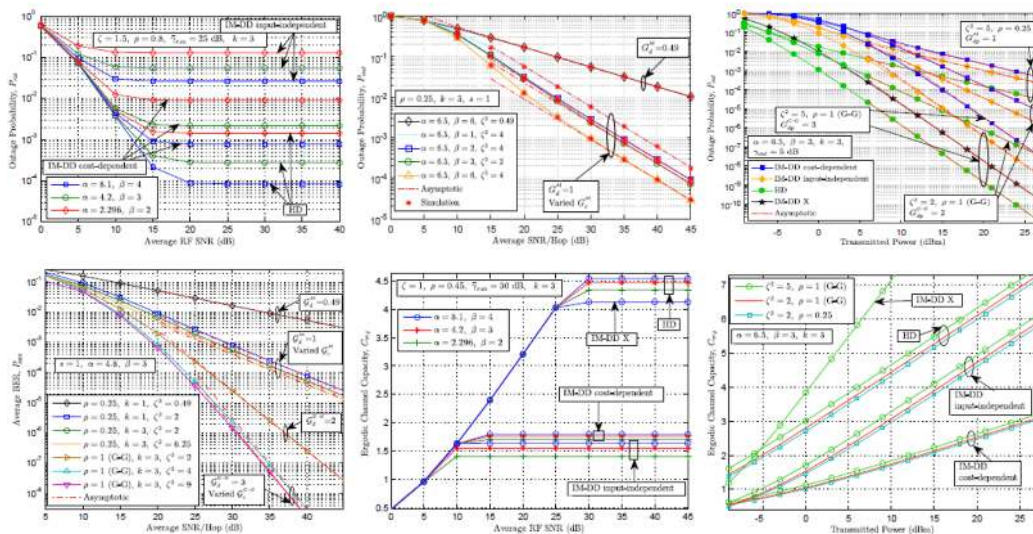# Precise Performance Analysis of Dual-Hop Mixed RF/Unified-FSO DF Relaying With Heterodyne Detection and Two IM-DD Channel Models

Omer Mahmoud Salih Al-Ebraheemy
Anas M. Salhab, *Senior Member, IEEE*
Anas Chaaban, *Senior Member, IEEE*
Salam A. Zummo, *Senior Member, IEEE*
Mohamed-Slim Alouini, *Fellow, IEEE*

Precise Performance Analysis of Dual-Hop Mixed RF/Unified-FSO DF Relaying With Heterodyne Detection and Two IM-DD Channel Models

Omer Mahmoud Salih Al-Ebraheemy [1]
Anas M. Salhab [1], *Senior Member, IEEE*,
Anas Chaaban [2], *Senior Member, IEEE*,
Salam A. Zummo [1], *Senior Member, IEEE*,
and Mohamed-Slim Alouini [3], *Fellow, IEEE*

[1] Department of Electrical Engineering, King Fahd University of Petroleum and Minerals, Dhahran 31261, Saudi Arabia
[2] School of Engineering, University of British Columbia, Kelowna BC V6T 1Z4, Canada
[3] CEMSE Division, King Abdullah University of Science and Technology, Thuwal 23955, Saudi Arabia

Abstract: This paper provides precise performance analysis of the dual-hop mixed radio frequency (RF)/unified free space optical (FSO) decode-and-forward (DF) relaying system, in which the heterodyne detection and the intensity modulation-direct detection (IM-DD) are taken into account for FSO detection. To this end, we derive closed-form expressions for the outage probability, average bit error rate (BER), and the ergodic channel capacity of this system. In this analysis, we utilize, for the first time as per our knowledge, a precise channel capacity result for the IM-DD channel. Moreover, this is the first time that not only the (IM-DD input-independent) but also the (IM-DD cost-dependent) additive white Gaussian noise (AWGN) channel is considered in such system analyses. Additionally in this study, we assume that the first hop (RF link) follows Nakagami-m fading, and the second hop (FSO link) follows Málaga ($\mathcal{M}$) turbulence with pointing errors. These fading and turbulence models contain other models (such as Rayleigh and Gamma–Gamma) as special cases, thus, our analyses can be seen as a generalized one from the RF and FSO fading models point of view. Also, in BER derivation, we assume that the modulation schemes in the two hops can be different, since not all modulation schemes are suitable for IM-DD FSO links. In addition, the system performance is investigated asymptotically at high signal to noise ratios. This investigation leads to new nonreported coding gain and diversity order analyses of such system. Interestingly, we find that in the FSO hop, at high transmitted powers, all the considered FSO detectors result in the same diversity order. Furthermore, we provide simulation results that verify the accuracy of the obtained analytical and asymptotic expressions.

Index Terms: Mixed RF/FSO relay network, Nakagami-m fading, Málaga ($\mathcal{M}$) fading, intensity modulation-direct detection, IM-DD, heterodyne detection, HD, decode-and-forward, DF.

1. Introduction

1.1 Background and Motivation

The distinctive features of free space optical (FSO) communications, such as its license-free spectrum, quick deployment, low power consumption, sturdiness to RF interference and high security, give rise to a growing interest on the research in this field recently, see [2], [3] and references therein. One of the main challenges in FSO communications is that it can offer transmission only over relatively short distance due to some optical propagation limiting factors. These factors are basically the atmospheric path loss, atmospheric turbulence-induced fading, beam dispersion, the pointing instability in wind, and the sensitivity to weather conditions such as snow, cloud, fog, and smog. However, an energy efficient method to overcome this problem and to extend the coverage area in wireless communications is to use relay networks. In these networks, a relay or a group of relays are utilized to support a source node in transmitting data to a destination.

Therefore, FSO relay networks have gained a considerable research attention in literature. For example the performance of FSO relaying schemes was studied in [4]–[7]. On the other hand, the dual-hop mixed RF/FSO relaying performance was investigated in [8]–[18]. Moreover recently, the performance of triple-hop mixed RF/FSO/RF relaying was analyzed in [19]–[21].

Namely, in single relay systems, the performance of FSO relay network was investigated in [4], [5] using log-normal fading model which is commonly used in modeling the FSO link in weak atmospheric turbulence situations. Specifically, the work in [4] studied the outage probability of the decode-and-forward (DF) and amplify-and-forward (AF) FSO relaying network under the existence of the direct source-to-destination link. Alternatively, in [6], [7] the FSO relay network performance was investigated using Gamma-Gamma (G-G) fading channel model which is more accurate and can be used in modeling the FSO link in strong and weak turbulence situations. Specifically, in [7], closed-form expressions were derived for the outage and symbol error (SER) probabilities of the two way FSO relay networks.

One of the very important configurations in the literature is the dual-hop mixed RF/FSO relay network. The significance of this configuration comes from its worthy applications such as in mobile cellular systems and femtocells networks in which the mobile stations (sources) are multiplexed to transmit their information to a relay station through an RF connection in the first hop, and in the second hop the information is forwarded by the relay to the macro base station (destination) through an FSO connection. Such mixed relaying configuration economically saves the resources by preventing unnecessary expensive installation for optical fibres, for example in suburban and downtown areas, and simultaneously saves the RF spectrum while providing high data rates by utilizing the FSO connection.

Thence, in [8] closed-form expressions were developed for the outage probability, bit error rate (BER), and channel capacity of AF variable gain mixed RF/FSO dual-hop relay scheme. It was assumed there that the RF link follows Rayleigh fading while the FSO link follows G-G fading with pointing error, and both intensity modulation-direct detection (IM-DD) as well as heterodyne detection (HD) were considered for FSO detection. A similar system to that in [8] was studied in terms of its SER in [9] for AF fixed-gain mixed shadowed-Rician/G-G without pointing error. Another similar scheme to the one in [8] was investigated in [10] and [11] for fixed-gain AF relaying, where in [11] a direct link was considered from the source to the destination. Additionally, similar schemes to those in [10] and [11] were analyzed in [12] and [13], respectively, but for Nakagami-m faded RF link. Also, an analogous scheme to these ones was studied in [14] for fixed and variable gain AF mixed Nakagami-m/G-G relaying. Moreover, a scheme like the one in [8] was inspected in [15], but this time for multiusers (sources) opportunistic scheduling. In addition, the BER and outage probability for AF (fixed and variable gain) mixed RF/FSO schemes were investigated in [16] assuming Nakagami-m and double generalized Gamma fading models for the RF and FSO channels, respectively, and considering the co-channel interference, existence of the direct RF link, and the pointing error.

However, a common considerable problem in mixed RF/FSO AF schemes, as in [8]–[16], is that they do not satisfy the non-negativity of the FSO IM-DD transmitted signal, even if subcarrier

intensity modulation (SIM) is utilized in some of them. Particularly, in these AF schemes the relay receives an unbounded bipolar signal, which can not be made positive, for the sake of IM-DD transmission, by mere amplification and/or applying a DC bias. Therefore, the mathematical model and the results of the above AF works do not reflect the correct performance of those mixed RF/FSO AF systems when IM-DD is used. This non-negativity of the IM-DD transmitted signal can be satisfied by using a DF mixed RF/FSO relaying system like the one employed in [17], [18]. Namely, in [18] the performance of multiuser mixed RF/FSO dual hop DF relaying system was investigated using V-BLAST technique, IM-DD, and G-G fading channels with pointing error.

Nevertheless, the problem in the works in [17], [18] is that they did not use the correct capacity results for IM-DD channel. Instead, they used the well-known Shannon's AWGN channel capacity [22] which does not apply for IM-DD systems , because it does not consider the non-negativity constraint in the IM-DD transmitted signal.

Thus, due to the significance of the mixed RF/FSO relaying and to overcome the above mentioned problems in its analysis, we investigate in this paper the performance of dual-hop mixed RF/unified FSO DF relaying system, where both HD and IM-DD are considered in the FSO hop. To this end, we derive closed-form expressions for the outage probability, BER, and ergodic channel capacity for this scheme.

1.2 Contributions

In this study the main contributions are:

- We correctly utilize, for the first time to the best of our knowledge, in such system outage and capacity analysis, a precise channel capacity approximation for the IM-DD channel deduced in [23]–[27]. This precise approximation is tight at high-SNR, and hence it can serve as the channel capacity in that regime. Consequently, this work presents precise quantitative comparison between HD and IM-DD performances, and thus helps the designers in deciding whether to deploy HD (higher rate) or IM-DD (lower cost/complexity).

- Moreover, to the best of our knowledge, this is the first time that not only the IM-DD input-independent but also the IM-DD cost-dependent AWGN channel is taken into account in such system analyses. The difference between these two IM-DD channel models is in the AWGN variance which is independent of the input signal in the first model, while in the second model it is proportional to the constraint (cost) of the input signal (optical average power constraint here). Also, it is worthy to mention that the IM-DD input-independent AWGN channel model [23], [25] is only applicable wherever the thermal noise dominates the total receiver noise which is the case in the receiver that uses the PIN-photodiode or in case of low optical powers. Alternatively, IM-DD cost-dependent AWGN channel model [26], [27] is useful when the shot-noise dominates the total receiver noise which is the case in the receiver based on the avalanche photodiode (APD), or in case of high optical powers.

- Also, we run the BER analysis under the assumption that the two hops do not necessarily use the same modulation scheme. This assumption is valid in the DF relaying schemes, which is the case in our work, and it is one of their advantages. Especially, this is very important in mixed RF/ FSO relaying as not all modulation schemes are suitable for IM-DD FSO communications. Specifically, in the IM-DD systems we modulate the optical intensity (non-negative quantity) which does not have a phase, and hence all kinds of phase modulations are not applicable there.

- Additionally, the performance of the system is studied asymptotically at the high SNRs regime. This asymptotic study results in new non-reported coding gain and diversity order analyses of such system. Interestingly, we find that in the FSO hop, based on the average SNRs, the HD or IM-DD cost-dependent results in the same diversity order which is twice the one of IM-DD input-independent. However, each FSO detector has a distinct relation between its average SNR and the transmitted power, thus based on the transmitted power all the FSO detectors result in the same diversity order, whereas the coding gain is different for each FSO detector.

Fig. 1. Mixed RF/FSO dual-hop DF relaying system.

- Furthermore, at high transmitted powers, we find that, in the FSO hop, the ergodic capacities pre-logs for HD and IM-DD input-independent are identical and equal twice the one of the IM-DD cost-dependent.
- All the above analysis is done in a unified manner for the FSO hop which combines HD, IM-DD input-independent, and (for the first time) IM-DD cost-dependent in a unified expression for each statistical characteristic or performance indicator. Note that obtaining these unified expressions is not straightforward.

In doing this work, we assume that the FSO link follows Málaga ($\mathcal{M}$) fading with pointing errors, whereas the RF link follows Nakagami-m fading which can be used to model the LOS transmission (see e.g. [14], [28]) between the source and relay. Note that Nakagami-m also models the non LOS (NLOS) transmission (i.e., Rayleigh fading) as a special case. Also, notice that the $\mathcal{M}$ fading model contains other FSO fading models (including G-G) as special cases. Therefore, our performance analyses can be seen as a generalized one from the FSO and RF fading models point of view.

The remainder of this paper is arranged as follows. The system model is presented in Section 2. Section 3 analyzes the system performance. Numerical and simulation results are carried out and discussed in Section 4, these results confirm the accuracy of the derived analytical and asymptotic expressions. Finally, conclusions are provided in Section 5.

2. System and Channel Models

The system under study is a mixed RF/FSO dual-hop relaying scheme which consists of a source S, a DF relay R, and a destination D as shown in Fig. 1. The source communicates with the relay via an RF channel and the relay communicates with the destination via an FSO channel. The direct S–D link is assumed to be infeasible. The transmission from S to D takes place over two phases (i.e., two channel uses): S $\rightarrow$ R and R $\rightarrow$ D. In the first phase, the RF signal received from S at R can be represented as

$$y_{\text{RF}} = \sqrt{P_s}\, h_{\text{RF}}\, x_{\text{RF}} + n_r, \tag{1}$$

where x_{RF} is the transmitted signal from S with $\mathbb{E}\{|x_{\text{RF}}|^2\} = 1$, P_s is the transmitted power from S, h_{RF} is the coefficient of the fading channel from S to R, $n_r \sim \mathcal{CN}(0, N_0)$ is an AWGN, and $\mathbb{E}\{\cdot\}$ denotes the expectation operator. Hence, the SNR at R can be expressed as $\gamma_{\text{RF}} = \frac{P_s}{N_0}|h_{\text{RF}}|^2$. In this work we assume that the RF channel coefficient follows Nakagami-m fading model, where we use k to represent the parameter m and restrict it to be an integer value. Thus, the probability density function (pdf) of γ_{RF} is given by [28]

$$f_{\gamma_{\text{RF}}}(\gamma) = \left(\frac{k}{\bar{\gamma}_{\text{RF}}}\right)^k \frac{\gamma^{k-1}}{(k-1)!} \exp\left(-\frac{k}{\bar{\gamma}_{\text{RF}}}\gamma\right), \tag{2}$$

where $\bar{\gamma}_{\text{RF}}$ is the average received RF SNR. Namely, $\bar{\gamma}_{\text{RF}} = \frac{P_s}{N_0}\mathbb{E}\{|h_{\text{RF}}|^2\} = \frac{P_s}{N_0}\Omega_{\text{RF}}$, where we define Ω_{RF} as $\Omega_{\text{RF}} = \mathbb{E}\{|h_{\text{RF}}|^2\}$. Note that $(P_s\Omega_{\text{RF}})$ designates the average received power at R, and hence Ω_{RF} can represent the multiplication of the RF link losses (L_{RF}), gains (K_{RF}) and design margins (M_{RF}). These losses include RF transmitter losses (Lt_{RF}), RF receiver losses (Lr_{RF}), path loss (Ls_{RF}) (This loss is constant for a given link distance and weather condition), etc. Thus, for example, we can have $\Omega_{\text{RF}} = L_{\text{RF}} K_{\text{RF}} M_{\text{RF}} = Lt_{\text{RF}} Lr_{\text{RF}} Ls_{\text{RF}} K_{\text{RF}} M_{\text{RF}}$.

It is worthy to say that when ($k = 1$) the RF channel model reduces to the Rayleigh fading model as a special case.

After receiving and decoding the signal, R forwards it to the destination in the second transmission phase. Let x_{HD} and x_{IMDD} denote the transmitted signal to D from R in case of HD and IM-DD, respectively, with average power constraints $\mathbb{E}\{|x_{\text{HD}}|^2\} = 1$ and $\mathbb{E}\{x_{\text{IMDD}}\} = 1$. Notice that the average power constraint in the IM-DD is on the expected value of the signal and not on its square because the signal in this case represents an optical intensity. Consequently, the received FSO signal from R at D in case of HD and IM-DD can be, respectively, represented as

$$y_{\text{HD}} = \sqrt{P_r}\, g_{\text{FSO}}\, x_{\text{HD}} + n_{\text{HD}}, \tag{3}$$

$$y_{\text{IMDD}} = P_r\, I_{\text{FSO}}\, x_{\text{IMDD}} + n_{\text{IMDD}}, \tag{4}$$

where P_r is R transmitted power, g_{FSO} and $I_{\text{FSO}} = |g_{\text{FSO}}|^2$ represent the fluctuation in the received electric field and irradiance, respectively. This fluctuation is due to the atmospheric turbulence and pointing error in the $R \rightarrow D$ link. In (3), the noise $n_{\text{HD}} \sim \mathcal{CN}(0, N_{\text{HD}})$ is a complex AWGN. Whereas in (4), the noise n_{IMDD} is a real AWGN where $n_{\text{IMDD}} \sim \mathcal{N}(0, N_{\text{IMDD}})$ for the case of IM-DD input-independent AWGN channel, and $n_{\text{IMDD}} \sim \mathcal{N}(0, 2P_r I_{\text{FSO}} N_{\text{HD}} \mathbb{E}\{x_{\text{IMDD}}\})$ for the case of IM-DD cost-dependent AWGN channel assuming relatively high P_r as compared to the thermal plus background noise power. For the details of the HD and the two types of the IM-DD and their noise variances, the reader is referred to [26], [27]. Therefore the SNR at D, upon which the outage, BER, and capacity are based, is introduced as follows for HD, IM-DD input-independent, and IM-DD cost-dependent, respectively,

$$\gamma_{\text{HD}} = \frac{P_r |g_{\text{FSO}}|^2}{N_{\text{HD}}} \mathbb{E}\{|x_{\text{HD}}|^2\} = \frac{P_r I_{\text{FSO}}}{N_{\text{HD}}}, \; \gamma_{\text{IMDD}_{indp}} = \frac{P_r^2 I_{\text{FSO}}^2}{N_{\text{IMDD}}} \mathbb{E}^2\{x_{\text{IMDD}}\} = \frac{P_r^2 I_{\text{FSO}}^2}{N_{\text{IMDD}}},$$

$$\gamma_{\text{IMDD}_{cost}} = \frac{P_r^2 I_{\text{FSO}}^2 \mathbb{E}^2\{x_{\text{IMDD}}\}}{2 P_r I_{\text{FSO}} N_{\text{HD}} \mathbb{E}\{x_{\text{IMDD}}\}} = \frac{P_r I_{\text{FSO}}}{2 N_{\text{HD}}}. \tag{5}$$

In this paper, we assume that the $R \rightarrow D$ FSO channel experiences $\mathcal{M}$ fading model with the pointing errors. In developing the $\mathcal{M}$ fading model in [29], it is assumed that the received signal consists of a LOS component (U_L), a component scattered by eddies on the propagation axis and coupled to the LOS (U_S^C), and a component scattered by off-axis eddies (U_S^G) which is statistically independent from U_L and U_S^C. So as a result of adopting the $\mathcal{M}$ fading model with pointing errors for the FSO link, the pdf of I_{FSO} is given by [30, Eq. (21)]

$$f_{I_{\text{FSO}}}^{\mathcal{M}}(I) = \frac{\zeta^2 A}{2I} \sum_{m=1}^{\beta} b_m G_{1,3}^{3,0} \left[\frac{\alpha\beta}{g\beta + \Omega'} \frac{I}{A_0} \middle| \begin{matrix} \zeta^2+1 \\ \zeta^2, \alpha, m \end{matrix} \right], \tag{6}$$

where

$$A = \frac{2\alpha^{\alpha/2}}{g^{1+\alpha/2}\Gamma(\alpha)} \left(\frac{g\beta}{g\beta + \Omega'} \right)^{\beta+\alpha/2}, \quad b_m = a_m \left[\alpha\beta / \left(g\beta + \Omega' \right) \right]^{-(\alpha+m)/2},$$

$$a_m = \binom{\beta-1}{m-1} \frac{(g\beta + \Omega')^{1-m/2}}{(m-1)!} \left(\frac{\Omega'}{g} \right)^{m-1} \left(\frac{\alpha}{\beta} \right)^{m/2},$$

α is a positive parameter which represents the effective number of large-scale cells of the scattering (fluctuation) process, β is a natural number[1] which represents the amount of fading related to the effective number of small-scale cells of the fluctuation process,[2] $\Omega' = \Omega + 2b_0\rho + 2\sqrt{2b_0\rho\Omega} \cos(\Phi_A - \Phi_B)$ is the average power of the coherent contributions, $\Omega = \mathbb{E}\{|U_L|^2\}$, $\mathbb{E}\{|U_S^C|^2\} = 2b_0\rho$, Φ_A and Φ_B are the deterministic phases of the LOS and the coupled-to-LOS signal components, respectively,

---

[1] In this work we restrict β to be a natural number. This restriction leads to a closed-form expression with a finite summation ($\sum_{m=1}^{\beta}$) for the pdf of I_{FSO} as in (6), and hence more evident analytical tractability is assured. Also, due to the high degree of freedom of the $\mathcal{M}$ distribution, as shown in [29], the aforementioned restriction does not prevent it to offer an excellent fitting to the experimental data, in all turbulent conditions, without the need for the infinite summation ($\sum_{m=1}^{\infty}$) which appears in the pdf of I_{FSO}, as given by [30, Eq. (23)], in the generalized case when β is a real number.

[2] The fading parameters α and β are related to the atmospheric turbulence conditions (Rytov variance) with lower values generally representing severe (strong) atmospheric turbulence conditions having the other parameters fixed.

$2b_0 = \mathbb{E}\{|U_S^C|^2 + |U_S^G|^2\}$ is the total average power of the scattered components, $g = \mathbb{E}\{|U_S^G|^2\} = 2b_0(1 - \rho)$, the parameter $0 \leq \rho \leq 1$ indicates the amount of the scattered power coupled to the LOS,[3] ζ is the ratio of the equivalent beam radius to the pointing error displacement standard deviation (jitter) at the receiver (i.e., $\zeta \to \infty$, denotes the non-pointing error case),[4] A_0 is a constant which defines the pointing loss (or generally the FSO link losses and design margins), $\Gamma(\cdot)$ is the Gamma function as defined in [32, Eq. (8.310)], and G[·] is the Meijer's G-function as defined in [32, Eq. (9.301)].

It is worthy to mention that, in general the constant A_0 can represent the multiplication of the FSO link losses (L_{FSO}), gains (K_{FSO}) and design margins (M_{FSO}). These losses include FSO transmitter losses (Lt_{FSO}), FSO receiver losses (Lr_{FSO}), pointing loss (Lp_{FSO}), path loss (Ls_{FSO}) (This loss is constant for a given link distance and weather condition), etc. Thence, for example, we can have $A_0 = L_{FSO} K_{FSO} M_{FSO} = Lt_{FSO} Lr_{FSO} Lp_{FSO} Ls_{FSO} K_{FSO} M_{FSO}$.

From the pdf in (6) (i.e., $f_{I_{FSO}}^{\mathcal{M}}(I)$) and by using random variable transformation, we obtain the pdfs of the SNRs in (5) in the following unified form

$$f_{\gamma_{FSO}}^{\mathcal{M}}(\gamma) = \frac{\zeta^2 A}{2^s \gamma} \sum_{m=1}^{\beta} b_m G_{1,3}^{3,0}\left[B\left(\frac{w\gamma}{\mu_s}\right)^{1/s} \Big|_{\zeta^2,\alpha,m}^{\zeta^2+1} \right], \tag{7}$$

where γ_{FSO} is used to indicate the unified SNR of the FSO link, $B = \zeta^2 \alpha \beta (g + \Omega')/[(\zeta^2 + 1)(g\beta + \Omega')]$, s and w are the parameters that identify the type of the FSO detection, i.e., $(s, w)=(1,1)$, $(2,1)$ or $(1,2)$ for HD, IM-DD input-independent, and IM-DD cost-dependent respectively, and where $\mu_1 \triangleq P_r \mathbb{E}\{I_{FSO}\}/N_{HD} = A_0 P_r \zeta^2 (g + \Omega')/[(\zeta^2 + 1)N_{HD}]$, and for normalization purposes $\mu_2 \triangleq P_r^2 \mathbb{E}^2\{I_{FSO}\}/N_{IMDD}$ as previously defined in [33] and references therein. This definition results in $\mu_2 = A_0^2 P_r^2 \zeta^4 (g + \Omega')^2/[(\zeta^2 + 1)^2 N_{IMDD}]$. From these expressions of μ_1, μ_2, and (5), it is clear that μ_s is proportional to the average of the unified FSO SNR ($\bar{\gamma}_{FSO}$). Specifically, $\mu_1 = \bar{\gamma}_{HD} = 2\bar{\gamma}_{IMDD_{cost}}$, however $\mu_2 = \bar{\gamma}_{IMDD_{indp}} \frac{\mathbb{E}^2\{I_{FSO}\}}{\mathbb{E}\{I_{FSO}^2\}} = \frac{\zeta^2(\zeta^2+1)^{-2}(\zeta^2+2)(g+\Omega')^2}{\alpha^{-1}(\alpha+1)[2g(g+2\Omega')+\Omega'^2(1+1/\beta)]} \bar{\gamma}_{IMDD_{indp}}$.[5]

Notice that when $\rho = 1$ (i.e., $g = 0$), we get $A b_m = 2/(\Gamma(\alpha)\Gamma(\beta))$ for $m = \beta$ and $A b_m = 0$ for all other m. Thus, when $\rho = 1$, and $\Omega' = 1$ (for normalization), the pdf $f_{I_{FSO}}^{\mathcal{M}}(I)$ in (6) turns to the G-G distribution with pointing error, given by [34, Eq. (1)], as a special case. Actually, having $\rho = 1$ means that the power $\mathbb{E}\{|U_S^G|^2\} \triangleq g = 0$, i.e., in the G-G fading channel model, the received signal component scattered by off-axis eddies (U_S^G) is neglected. Hence, by setting $\Omega' = 1$ and $\rho = 1$ in (7), the unified pdf of the FSO SNR in the G-G fading with pointing error can be expressed as

$$f_{\gamma_{FSO}}^{G-G}(\gamma) = \frac{\zeta^2}{s\gamma\Gamma(\alpha)\Gamma(\beta)} G_{1,3}^{3,0}\left[\frac{\zeta^2 \alpha \beta}{(\zeta^2 + 1)} \left(\frac{w\gamma}{\mu_s}\right)^{1/s} \Big|_{\zeta^2,\alpha,\beta}^{\zeta^2+1} \right]. \tag{8}$$

3. System Performance Analysis

3.1 Outage Probability

The outage probability (P_{out}) is an important performance metric in slow fading channels which are the channels in most RF and FSO systems [3], [35] including the system here. It is defined, as in [35], by $P_{out} = \Pr[C < R]$, where $\Pr[.]$ indicates the probability operator, R is the end-to-end (e2e) desired data rate in bits/channel-use, C is a function on the random equivalent-SNR of the e2e channel. Therefore, C is a random variable and its realization represents the e2e channel capacity given the corresponding realization of the e2e channel equivalent-SNR. As in any dual-hop DF relaying system, in the system under study, the event of the outage occurs if either the first hop or the second hop is in outage, i.e., the e2e outage event is the union of the outage events of the two

---

[3]The details of the $\mathcal{M}$ distribution and the generation of its random variable can be drawn out from [29, Eqs. (13–21)].
[4]For more details on the pointing error model, the reader is referred to [31].
[5]$\mathbb{E}\{I_{FSO}\}$ and $\mathbb{E}\{I_{FSO}^2\}$ are derived from [30, Eq. (33)].

hops. Hence the outage probability in our system is given by [6]

$$P_{out} = \Pr\left[C_{RF} < 2R \bigcup C_{FSO} < 2R\right], \tag{9}$$

$$= \Pr\left[\frac{1}{2}\min\left[C_{RF}, C_{FSO}\right] < R\right], \tag{10}$$

where C_{RF} and C_{FSO} are related to the channel capacity of the first hop (RF link) and the second hop (FSO link), respectively.

Specifically, C_{RF} is a function on the random SNR of the first hop. Hence, C_{RF} is a random variable whose realization represents the channel capacity of the first hop given the corresponding realization of the first hop SNR (γ_{RF}). However, given γ_{RF}, the first hop is an AWGN channel as expressed in (1). So, using the expression of the AWGN channel capacity, given in [22], results in[7]

$$C_{RF} = \log(1 + \gamma_{RF}). \tag{11}$$

On the other hand, C_{FSO} is a function on the random SNR of the second hop, and hence it is also a random variable. Moreover, in case of HD the realization of C_{FSO} represents the channel capacity of the second hop given the corresponding realization of the second hop SNR (γ_{HD}). Alternatively, in case of IM-DD we relax the manner and let the realization of C_{FSO} represents an excellent approximation (just above the lower bound)[8] of the channel capacity of the second hop given the corresponding realization of the second hop SNR ($\gamma_{IMDD_{indp}}$ or $\gamma_{IMDD_{cost}}$). However, given γ_{HD}, $\gamma_{IMDD_{indp}}$ or $\gamma_{IMDD_{cost}}$ the second hop is, respectively, an AWGN channel, IM-DD input-independent AWGN channel, or IM-DD cost-dependent AWGN channel as represented by (3) or (4). Hence, using the AWGN channel capacity expression [22] and the approximations of the two IM-DD AWGN channel capacities [23], [27] results in

$$C_{FSO} = \begin{cases} \log\left(1 + \gamma_{HD}\right) & \text{for HD} \\ \log\left(1 + \sqrt{\frac{e}{2\pi}\gamma_{IMDD_{indp}}}\right) & \text{for IM-DD input-independent} \\ \log\left(1 + \sqrt{\frac{e}{2\pi}\gamma_{IMDD_{cost}}}\right) & \text{for IM-DD cost-dependent} \end{cases}, \tag{12}$$

or in a unified form

$$C_{FSO} = \log(1 + \gamma_{FSO}^{\text{eff}}), \tag{13}$$

where $\gamma_{FSO}^{\text{eff}}$ is used to indicate the unified effective SNR of the FSO connection, i.e., $\gamma_{FSO}^{\text{eff}}$ equals to either γ_{HD}, $\sqrt{\frac{e}{2\pi}\gamma_{IMDD_{indp}}}$, or $\sqrt{\frac{e}{2\pi}\gamma_{IMDD_{cost}}}$ based on the used FSO transmission scheme. Due to its importance in what follows, let us calculate the pdf of $\gamma_{FSO}^{\text{eff}}$. From $f_{I_{FSO}}^{\mathcal{M}}(I)$ in (6), with the help of (5), and by using random variable transformation, the pdf of $\gamma_{FSO}^{\text{eff}}$ can be given in a unified form as

$$f_{\gamma_{FSO}^{\text{eff}}}^{\mathcal{M}}(\gamma) = \frac{w\,\xi^2 A}{2\,\gamma}\sum_{m=1}^{\beta} b_m G_{1,3}^{3,0}\left[B\left(\gamma/c\right)^w \frac{1}{\mu_s^{1/s}}\,\bigg|\,\begin{matrix}\xi^2+1\\\xi^2,\alpha,m\end{matrix}\right], \tag{14}$$

where $c = 1$, $\sqrt{\frac{e}{2\pi}}$, or $\sqrt{\frac{e}{4\pi}}$ for HD, IM-DD input-independent, or IM-DD cost-dependent, respectively, and the rest of parameters are as in (6) and (7). Note that by setting $\Omega' = 1$ and $\rho = 1$ in (14), we get the pdf of $\gamma_{FSO}^{\text{eff}}$ in the special case of G-G fading with pointing error as follows

$$f_{\gamma_{FSO}^{\text{eff}}}^{\text{G-G}}(\gamma) = \frac{w\,\xi^2}{\gamma\Gamma(\alpha)\Gamma(\beta)}G_{1,3}^{3,0}\left[\frac{\xi^2\alpha\beta\left(\gamma/c\right)^w}{(\xi^2+1)\,\mu_s^{1/s}}\,\bigg|\,\begin{matrix}\xi^2+1\\\xi^2,\alpha,\beta\end{matrix}\right]. \tag{15}$$

---

[6]R is the e2e desired transmission rate in bits/channel-use. Also, here the desired rates of the two hops are assumed equal, and hence the factor 2 is due to the assumption that the e2e transmission (from S to D) happens over two equal phases (i.e., two equal channel uses) which means that each hop rate is twice the e2e rate.

[7]In this paper, unless otherwise specified, the log base is 2.

[8]We use this approx. (just above the lower bound) because the IM-DD channel capacity is yet unknown in closed-form [25]. However, this approx. is very tight at high-SNR, and hence it can serve as the IM-DD channel capacity in that regime.

Now let's go back to P_{out} and substitute (11) and (13) in (10) to get

$$P_{out} = \Pr\left[\min\left[\gamma_{\mathrm{RF}}\,,\,\gamma_{\mathrm{FSO}}^{\mathrm{eff}}\right] < (2^{2R} - 1)\right]. \tag{16}$$

From (16) we realize that P_{out} is nothing but the cumulative distribution function (CDF) of $\gamma_{eq} \triangleq \min\left[\gamma_{\mathrm{RF}}\,,\,\gamma_{\mathrm{FSO}}^{\mathrm{eff}}\right]$ evaluated at $\gamma_{out} \triangleq (2^{2R} - 1)$, this CDF, and hence P_{out}, can be expressed as [36]

$$P_{out} = F_{\gamma_{eq}}(\gamma_{out}) = F_{\gamma_{\mathrm{RF}}}(\gamma_{out}) + F_{\gamma_{\mathrm{FSO}}^{\mathrm{eff}}}^{\mathcal{M}}(\gamma_{out}) - F_{\gamma_{\mathrm{RF}}}(\gamma_{out})\,F_{\gamma_{\mathrm{FSO}}^{\mathrm{eff}}}^{\mathcal{M}}(\gamma_{out}), \tag{17}$$

where $F_{\gamma_{\mathrm{RF}}}(\gamma_{out})$ and $F_{\gamma_{\mathrm{FSO}}^{\mathrm{eff}}}^{\mathcal{M}}(\gamma_{out})$ are the CDFs of γ_{RF} and $\gamma_{\mathrm{FSO}}^{\mathrm{eff}}$, respectively. These CDFs are, respectively, given, by integrating their corresponding pdfs in (2) and (14) with respect to γ, as follows

$$F_{\gamma_{\mathrm{RF}}}(\gamma) = 1 - \exp\left(-\frac{k\gamma}{\bar{\gamma}_{\mathrm{RF}}}\right)\sum_{i=0}^{k-1}\frac{1}{i!}\left(\frac{k\gamma}{\bar{\gamma}_{\mathrm{RF}}}\right)^i, \tag{18}$$

$$F_{\gamma_{\mathrm{FSO}}^{\mathrm{eff}}}^{\mathcal{M}}(\gamma) = \frac{\xi^2 A}{2}\sum_{m=1}^{\beta} b_m G_{2,4}^{3,1}\left[\frac{B\,(\gamma/c)^w}{\mu_s^{1/s}}\,\bigg|\,\begin{matrix}1,\xi^2+1\\\xi^2,\alpha,m,0\end{matrix}\right]. \tag{19}$$

Next, by substituting the CDFs (18) and (19) in (17), and after simple algebraic manipulations, we obtain

$$P_{out} = F_{\gamma_{eq}}(\gamma_{out}) = 1 - \left(\exp\left(-\frac{k\gamma_{out}}{\bar{\gamma}_{\mathrm{RF}}}\right)\sum_{i=0}^{k-1}\frac{1}{i!}\left(\frac{k\gamma_{out}}{\bar{\gamma}_{\mathrm{RF}}}\right)^i\right)\left(1 - \frac{\xi^2 A}{2}\sum_{m=1}^{\beta} b_m G_{2,4}^{3,1}\left[\frac{B\,(\gamma_{out}/c)^w}{\mu_s^{1/s}}\,\bigg|\,\begin{matrix}1,\xi^2+1\\\xi^2,\alpha,m,0\end{matrix}\right]\right). \tag{20}$$

Remember that the P_{out} in (20) is for the case of $\mathcal{M}$ fading in the FSO link. Alternatively, to obtain the P_{out} in the special case of G-G fading in the FSO link, the CDF $F_{\gamma_{\mathrm{FSO}}^{\mathrm{eff}}}^{\mathcal{M}}(\gamma)$ in (17) should be replaced by the CDF $F_{\gamma_{\mathrm{FSO}}^{\mathrm{eff}}}^{\mathrm{G\text{-}G}}(\gamma)$ which can be given, after integrating its pdf in (15), as follows

$$F_{\gamma_{\mathrm{FSO}}^{\mathrm{eff}}}^{\mathrm{G\text{-}G}}(\gamma) = \frac{\xi^2}{\Gamma(\alpha)\Gamma(\beta)}G_{2,4}^{3,1}\left[\frac{\xi^2\alpha\beta\,(\gamma/c)^w}{(\xi^2+1)\,\mu_s^{1/s}}\,\bigg|\,\begin{matrix}1,\xi^2+1\\\xi^2,\alpha,\beta,0\end{matrix}\right]. \tag{21}$$

3.2 Asymptotic Outage Probability

Due to the complexity of the derived expression in (20), it is not easy to know the impact of the different system parameters on its P_{out}. Thus, in this section we derive more simple (asymptotic) expression for the system outage probability at high SNRs regime. This asymptotic P_{out} provides more help in understanding and analyzing the performance of the system by offering some performance indicators of the system outage clearly in its expression.

Namely, in the high SNRs regime, the asymptotic outage probability can be normally given as $P_{out}^{(a)} \simeq (G_c\overline{\mathrm{SNR}})^{-G_d}$, where G_d and G_c are outage performance indicators which are, respectively, termed the diversity order and the coding gain related to the P_{out} of the system [28]. The diversity order G_d gives the slope of the log-log P_{out} versus average SNR plot in the high SNR regime, while $\log G_c$ gives the horizontal shift of this plot as compared to a benchmark outage probability plot of $(\overline{\mathrm{SNR}})^{-G_d}$.

Hence, to highlight G_d and G_c of our system, we need to reduce (20) to the typical $P_{out}^{(a)}$ expression. Consequently, we start by modifying (17) as follows: first we exchange the used CDFs by their asymptotic versions at the high SNRs regime, then we drop the last term since it is negligible at the high SNR. After these modifications, we get

$$P_{out}^{(a)} = F_{\gamma_{eq}}^{(a)}(\gamma_{out}) = F_{\gamma_{\mathrm{RF}}}^{(a)}(\gamma_{out}) + F_{\gamma_{\mathrm{FSO}}^{\mathrm{eff}}}^{\mathcal{M}(a)}(\gamma_{out}), \tag{22}$$

where $F_{\gamma_{RF}}^{(a)}(\gamma_{out})$ and $F_{\gamma_{FSO}^{eff}}^{\mathcal{M}(a)}(\gamma_{out})$ are, respectively, the asymptotic CDFs of γ_{RF} and γ_{FSO}^{eff} in the high SNRs regime. Next, we are left with determining these asymptotic CDFs. Let's start with $F_{\gamma_{RF}}^{(a)}(\gamma_{out})$ which is derived by first using the high SNR limit ($\lim_{\bar{\gamma}_{RF} \to \infty} \exp(-\frac{k\gamma}{\bar{\gamma}_{RF}}) = 1$) in (2) to get $f_{\gamma_{RF}}^{(a)}(\gamma) = (\frac{k}{\bar{\gamma}_{RF}})^k \frac{\gamma^{k-1}}{(k-1)!}$, then by integrating this asymptotic pdf we obtain

$$F_{\gamma_{RF}}^{(a)}(\gamma) = (k/\bar{\gamma}_{RF})^k \gamma^k/(k)! \ . \tag{23}$$

Then again to determine $F_{\gamma_{FSO}^{eff}}^{\mathcal{M}(a)}(\gamma_{out})$, we adjust (19) by applying [38, Eq. (07.34.06.0006.01)] which is the Meijer G-function series representation for $\frac{1}{\mu_s} \to 0$, i.e.,[9] $\bar{\gamma}_{FSO} \to \infty$ (high SNR). Doing this adjustment results in

$$F_{\gamma_{FSO}^{eff}}^{\mathcal{M}(a)}(\gamma) = \frac{\xi^2 A}{2} \sum_{m=1}^{\beta} b_m \sum_{l=1}^{3} \frac{\prod_{\substack{j=1,\\ j\neq l}}^{3} \Gamma\left(b_j' - b_l'\right)}{\Gamma\left(\xi^2 + 1 - b_l'\right) b_l'} \left(\frac{B(\gamma/c)^w}{\mu_s^{1/s}}\right)^{b_l'}, \tag{24}$$

where $b_1' = \xi^2$, $b_2' = \alpha$ and $b_3' = m$.[10] Moreover, (24) can be simplified more by keeping only the dominant term in the second summation ($\sum_{l=1}^{3}$) at high FSO SNR ($\frac{1}{\mu_s} \to 0$), i.e., the term which contains the minimum b_l' ($b_{min}' \triangleq \min[\xi^2, \alpha, m]$). By this simplification,[11] we get

$$F_{\gamma_{FSO}^{eff}}^{\mathcal{M}(a)}(\gamma) = \frac{\xi^2 A}{2} \sum_{m=1}^{\beta} b_m \frac{\prod_{j=1, b_j' \neq b_{min}'}^{3} \Gamma\left(b_j' - b_{min}'\right)}{\Gamma\left(\xi^2 + 1 - b_{min}'\right) b_{min}'} \left(\frac{B(\gamma/c)^w}{\mu_s^{1/s}}\right)^{b_{min}'}. \tag{25}$$

For the case of[12] $\rho \neq 1$, and by utilizing the definition of b_{min}', (25) can be expressed as

$$F_{\gamma_{FSO}^{eff}}^{\mathcal{M}(a)}(\gamma) = \Lambda \left(B(\gamma/c)^w/\mu_s^{1/s}\right)^{b_{min}''}, \tag{26}$$

where $b_{min}'' = \min[\xi^2, \alpha, 1]$, and

$$\Lambda \triangleq \begin{cases} \frac{\xi^2 A}{2} \sum_{m=1}^{\beta} b_m \frac{\prod_{j=1, b_j' \neq b_{min}'}^{3} \Gamma\left(b_j' - b_{min}'\right)}{\Gamma\left(\xi^2 + 1 - b_{min}'\right) b_{min}'} & \text{if} \quad \xi^2 \text{ or } \alpha < 1, \Rightarrow b_{min}' = \min[\xi^2, \alpha] \\ \frac{\xi^2 A}{2} b_1 \frac{\Gamma\left(\xi^2 - 1\right) \Gamma(\alpha - 1)}{\Gamma\left(\xi^2\right) \times 1} & \text{if} \quad \xi^2 \ \& \ \alpha > 1, \Rightarrow b_{min}' = 1 \end{cases}, \tag{27}$$

where in case of $b_{min}' = 1$, we keep only the first term ($m = 1$) in the summation with respect to m, because it is the dominating term in this summation at high FSO SNR.

Now upon substituting (23) and (26) in (22), we obtain

$$P_{out}^{(a)} = F_{\gamma_{eq}}^{(a)}(\gamma_{out}) = \left(\frac{(k!)^{1/k} \bar{\gamma}_{RF}}{k \gamma_{out}}\right)^{-k} + \left(\frac{\Lambda^{-s/b_{min}''} B^{-s} \mu_s}{(\gamma_{out}/c)^{ws}}\right)^{-b_{min}''/s}. \tag{28}$$

For the $P_{out}^{(a)}$ in (28), let us focus on two cases:

Case 1: The first hop dominates the system outage probability

---

[9]Because by definition, μ_s is proportional to $\bar{\gamma}_{FSO}$ (see the definitions after (7)).

[10]Note that [38, Eq.(07.34.06.0006.01)] requires that: $b_j' - b_l' \neq 0, \pm 1, \pm 2, \ldots$; $(j, l = 1, 2, 3; j \neq l)$. This condition can be fulfilled in all channels, without affecting the physical channel model, by adding different infinitesimal numbers (ϵ_l) to any b_l' which does not satisfy it. All the other conditions, given in [38], for [38, Eq.(07.34.06.0006.01)] to be valid are already satisfied here in our work.

[11]The deeper in high SNR regime we go, the more precise this simplification is. However generally speaking, in the beginning of the high SNR regime this simplification will be acceptable if b_{min}' is less than the other b_l''s by about 1 or more, otherwise the second summation in (24) ($\sum_{l=1}^{3}$) will be dominated by the terms which have the least b_l''s where the difference among these least b_l''s is less than about 1, and the difference between these least b_l''s and the other b_l''s is about 1 or more.

[12]The case of $\rho = 1$ (i.e., $g = 0$), in which $A b_m = 0$ for all m except $m = \beta$, is analyzed after (29b).

This is the case when the first summand in (28) is much larger than the second one, i.e., the 1st hop (RF link) is in worse condition than the 2nd hop (FSO link). Such case happens for example when the FSO link experiences relatively weak turbulence conditions and small pointing error, i.e., when α, β, and ζ have relatively big values. This case can also happen when the average RF SNR is relatively low.

By referring to the standard $P_{out}^{(a)}$ expression, it can be noted that, in this case, our considered system can accomplish a diversity order of k, $(G_d^{RF} = k)$, and a coding gain which is given by $G_c^{RF} = (k!)^{1/k}/(k\gamma_{out})$. So in this case the coding gain is a function of k and γ_{out}.

Case 2: The second hop dominates the system outage probability

In this case, the second summand in (28) is much bigger than the first one, i.e., the 2nd hop (FSO link) is in worse condition than the 1st hop (RF link) in this case. As an example, this case occurs when the FSO link suffers from relatively strong turbulence and significant pointing error, i.e., when α, β, and ζ have relatively small values. This case can also happen when the average RF SNR is relatively large.

Then again, by referring to the standard $P_{out}^{(a)}$ expression, it can be noted that, in this case, the accomplishable diversity order and coding gain of the system are, respectively, given by

$$G_d^{\mathcal{M}} = b_{min}''/s = \min[\zeta^2, \alpha, 1]/s, \tag{29a}$$

$$G_c^{\mathcal{M}} = \Lambda^{-s/b_{min}''} B^{-s}/(\gamma_{out}/c)^{ws}. \tag{29b}$$

Recall that the above $P_{out}^{(a)}$ in (28), and hence ((29a), (29b)) are when the FSO link encounters $\mathcal{M}$ fading with $\rho \neq 1$. Alternatively, to get the $P_{out}^{(a)}$ for the special case of G-G fading ($\rho = 1$) in the FSO link, the CDF $F_{\gamma_{FSO}^{eff}}^{\mathcal{M}(a)}(\gamma)$ in (22) should be changed by the CDF $F_{\gamma_{FSO}^{eff}}^{G\text{-}G(a)}(\gamma)$ which is given, by setting $\Omega' = 1$ (for normalization) and $\rho = 1$ in (25), as follows

$$F_{\gamma_{FSO}^{eff}}^{G\text{-}G(a)}(\gamma) = \left(\Delta^{1/b_{min}^{\star}} (\gamma/c)^w /\mu_s^{1/s} \right)^{b_{min}^{\star}}, \tag{30}$$

where $b_1^{\star} = \zeta^2$, $b_2^{\star} = \alpha$, $b_3^{\star} = \beta$, $b_{min}^{\star} = \min[\zeta^2, \alpha, \beta]$, and $\Delta \triangleq \frac{\zeta^2}{\Gamma(\alpha)\Gamma(\beta)} \left(\frac{\zeta^2 \alpha \beta}{\zeta^2+1} \right)^{b_{min}^{\star}} \frac{\prod_{j=1, b_j^{\star} \neq b_{min}^{\star}}^3 \Gamma\left(b_j^{\star} - b_{min}^{\star}\right)}{\Gamma\left(\zeta^2+1-b_{min}^{\star}\right) b_{min}^{\star}}$.

Consequently, by using (23) and (30), we get the $P_{out}^{(a)}$ for our system in the case of the mixed Nakagami-m/G-G fading as follows

$$P_{out}^{(a)} = F_{\gamma_{eq}}^{(a)}(\gamma_{out}) = F_{\gamma_{RF}}^{(a)}(\gamma_{out}) + F_{\gamma_{FSO}^{eff}}^{G\text{-}G(a)}(\gamma_{out}) \tag{31}$$

$$= \left(\frac{(k!)^{1/k} \bar{\gamma}_{RF}}{k\gamma_{out}} \right)^{-k} + \left(\frac{\Delta^{-s/b_{min}^{\star}} \mu_s}{(\gamma_{out}/c)^{ws}} \right)^{-b_{min}^{\star}/s}. \tag{32}$$

Here again for the $P_{out}^{(a)}$ in (32), we focus on the previous two cases. Regarding case 1, nothing is changed, and so we can conclude the same results as the previous ones. However, for case 2, i.e., when the 2nd summand dominates in (32), we can see that, related to P_{out}, our system accomplishes a coding gain and a diversity order which are, respectively, given by

$$G_c^{G\text{-}G} = \Delta^{-s/b_{min}^{\star}}/(\gamma_{out}/c)^{ws}, \tag{33a}$$

$$G_d^{G\text{-}G} = b_{min}^{\star}/s = \min[\zeta^2, \alpha, \beta]/s. \tag{33b}$$

It is worthy to notice that it is possible for $G_d^{G\text{-}G}$ to be greater than $1/s$, while this is not possible for $G_d^{\mathcal{M}}$. Another observation is that in the FSO hop, G_c is different for each FSO detector. However, based on the previous high SNRs analysis, using HD or IM-DD cost-dependent produces the same G_d which is twice the G_d of IM-DD input-independent. While, if the asymptotic analysis is based on high transmitted power regime, all these optical detectors will produce the same P_{out}-based diversity order (call it G_{dp}). To illustrate this consider the aforementioned "case 2", and by referring

to (28), (32), and recalling that μ_s is proportional to P_r^s (see definitions after (7)), it can be shown that, for all considered FSO detectors, we have

$$G_{dp}^{\mathcal{M}} = \min[\zeta^2, \alpha, 1], \tag{34a}$$

$$G_{dp}^{\text{G-G}} = \min[\zeta^2, \alpha, \beta]. \tag{34b}$$

Additional significant note here is that, to the best of our knowledge, no work in the literature (see e.g. [14], [17], [18], [37]) utilizes a precise IM-DD channel capacity approx., as (12), in such system outage analysis. Instead there has been an unsound adoption of the form $\left(\log\left(1 + \gamma_{\text{IMDD}_{indp}}\right)\right)$, let's denote it by IM-DD_capX, for IM-DD input-independent capacity in outage analysis. This leads to misconception in the comparison between HD and IM-DD, see Fig. 7. Hence, to overcome this we utilize Eqs. (12), (13) here to derive P_{out} and its asymptotic analysis.

Actually, by using the CDF of γ_{FSO} (given in (42) on next page) instead of the CDF of $\gamma_{\text{FSO}}^{\text{eff}}$ (given in (19)) in the outage analysis, it can be shown that, the unsound adoption of IM-DD_capX results in the same previous $G_d^{\mathcal{M}}$ and $G_d^{\text{G-G}}$ for IM-DD input-independent. Then again, by using (42) instead of (19) in P_{out} analysis, it can be seen that, the use of IM-DD_capX leads to the following P_{out}-based coding gains in case of $\mathcal{M}$ (with $\rho \neq 1$) and G-G ($\rho = 1$) fadings, respectively,

$$G_{c\_X}^{\mathcal{M}} = \Lambda^{-2/b_{min}''} B^{-2}/\gamma_{out}, \tag{35a}$$

$$G_{c\_X}^{\text{G-G}} = \Delta^{-2/b_{min}^{\star}}/\gamma_{out}. \tag{35b}$$

Therefore, by comparing (35a), (35b) with (29b), (33a) (when $s = 2$, $w = 1$, and $c = \sqrt{\frac{e}{2\pi}}$), we observe that there is a coding gain overestimation by using IM-DD_capX instead of our precise IM-DD input-independent capacity approx. (12). This overestimation in the P_{out}-based coding gain is given, in dB for both $\mathcal{M}$ (with $\rho \neq 1$) and G-G ($\rho = 1$), by

$$\delta G_c = 10\log_{10}(2\pi\gamma_{out}/e) = 10\log_{10}(\gamma_{out}) + 3.639 \text{ dB.} \tag{36}$$

The δG_c in (36) is based on high SNR analysis. However, by comparing the 2nd summands in (28), and (32) with a P_{out} of the form $(G_{cp}P_r)^{-G_{\Phi}}$, after recalling that μ_2 is proportional to P_r^2, it can be shown that, based on high Tx power regime, the aforementioned overestimation in G_c is given by

$$\delta G_{cp} = \delta G_c/2 = 5\log_{10}(\gamma_{out}) + 1.819 \text{ dB.} \tag{37}$$

3.3 Bit Error Rate

In general, for a dual-hop DF relaying scheme over independent fading channels, the average BER can be introduced as follows [39, Eq. (14)]

$$P_{BER} = P_{BER}^{hp1} + P_{BER}^{hp2} - 2P_{BER}^{hp1} P_{BER}^{hp2}, \tag{38}$$

where P_{BER}^{hp1} and P_{BER}^{hp2} are the average BERs for the first and second hop, respectively. In terms of their corresponding CDFs, these average BERs can be expressed as [40]

$$P_{BER}^{hp1} = \frac{a_1\sqrt{b_1}}{2\sqrt{\pi}} \int_0^\infty \frac{\exp(-b_1\gamma)}{\sqrt{\gamma}} F_{\gamma_{\text{RF}}}(\gamma)\, d\gamma, \tag{39}$$

$$P_{BER}^{hp2} = \frac{a_2\sqrt{b_2}}{2\sqrt{\pi}} \int_0^\infty \frac{\exp(-b_2\gamma)}{\sqrt{\gamma}} F_{\gamma_{\text{FSO}}}^{\mathcal{M}}(\gamma)\, d\gamma, \tag{40}$$

where a_1, b_1, a_2, and b_2 are the parameters which specify the modulation type in the corresponding hop.[13] For a possible list of the modulation types indicated by these parameters, the reader is

---

[13]Eqs. (39) and (40) represent the symbol error rate. So they give the BER in case of binary modulations, while they give an upper bound for the BER of M-ary modulations. Moreover if they are divided by the #bits/symbol, they will provide a lower bound for the BER of M-ary modulations which is an excellent BER approx. at high SNR when gray mapping is used [41].

referred to [40]. Now to obtain P_{BER}^{hp1}, we carry out the integration in (39), after substituting (18) in it, with the help of [32, Eq. (3.381.4)] to get

$$P_{BER}^{hp1} = \frac{a_1 \sqrt{b_1}}{2\sqrt{\pi}} \left[\frac{\Gamma(0.5)}{b_1^{0.5}} - \sum_{i=0}^{k-1} \left(\frac{k}{\bar{\gamma}_{RF}} \right)^i \frac{\Gamma(i+0.5)}{i!(b_1 + k/\bar{\gamma}_{RF})^{(i+0.5)}} \right]. \tag{41}$$

Alternatively, to solve the integral in (40) we need the CDF $F_{\gamma_{FSO}}^{\mathcal{M}}(\gamma)$ which can be given, by integrating its pdf in (7) with the help of [38, Eq.(07.34.21.0084.01)], as follows

$$F_{\gamma_{FSO}}^{\mathcal{M}}(\gamma) = D \sum_{m=1}^{\beta} c_m G_{s+1,3s+1}^{3s,1} \left[E \frac{\gamma}{\mu_s} \bigg|_{\mathbf{x}_2,\,0}^{1,\,\mathbf{x}_1} \right], \tag{42}$$

where $D = \zeta^2 A / [2^s (2\pi)^{s-1}]$, $c_m = b_{ms}^{\alpha+m-1}$, $E = B^s w / s^{2s}$, $\mathbf{x}_1 = \frac{\zeta^2+1}{s}, \dots \frac{\zeta^2+s}{s}$ includes s terms, and $\mathbf{x}_2 = \frac{\zeta^2}{s}, \dots \frac{\zeta^2+s-1}{s}, \frac{\alpha}{s}, \dots \frac{\alpha+s-1}{s}, \frac{m}{s}, \dots \frac{m+s-1}{s}$ includes $3s$ terms. Now the P_{BER}^{hp2} is given, after substituting (42) in (40), with the help of [32, Eq. (7.813.1)] as follows

$$P_{BER}^{hp2} = \frac{a_2 D}{2\sqrt{\pi}} \sum_{m=1}^{\beta} c_m G_{s+2,3s+1}^{3s,2} \left[\frac{E}{b_2\,\mu_s} \bigg|_{\mathbf{x}_2,\,0}^{0.5,\,1,\,\mathbf{x}_1} \right]. \tag{43}$$

Subsequently, upon substituting (41) and (43) in (38), we get

$$P_{BER} = \frac{a_1 \sqrt{b_1}}{2\sqrt{\pi}} \left[\frac{\Gamma(0.5)}{b_1^{0.5}} - \sum_{i=0}^{k-1} \left(\frac{k}{\bar{\gamma}_{RF}} \right)^i \frac{\Gamma(i+0.5)}{i!\,(b_1 + k/\bar{\gamma}_{RF})^{(i+0.5)}} \right] \left[1 - \frac{a_2 D}{\sqrt{\pi}} \sum_{m=1}^{\beta} c_m G_{s+2,3s+1}^{3s,2} \left[\frac{E}{b_2\,\mu_s} \bigg|_{\mathbf{x}_2,\,0}^{0.5,\,1,\,\mathbf{x}_1} \right] \right]$$

$$+ \frac{a_2 D}{2\sqrt{\pi}} \sum_{m=1}^{\beta} c_m G_{s+2,3s+1}^{3s,2} \left[\frac{E}{b_2\,\mu_s} \bigg|_{\mathbf{x}_2,\,0}^{0.5,\,1,\,\mathbf{x}_1} \right]. \tag{44}$$

Notice that the P_{BER}^{hp2} in (43), and hence the P_{BER} in (44), is when the FSO link (2nd hop) faces $\mathcal{M}$ fading. Nevertheless, the same previous procedures can be followed to attain the P_{BER}^{hp2}, and its related P_{BER}, for the G-G faded FSO link, however the CDF $F_{\gamma_{FSO}}^{\mathcal{M}}(\gamma)$ in (40) should be changed by $F_{\gamma_{FSO}}^{G\text{-}G}(\gamma)$ which is given, by setting $\Omega' = 1$ and $\rho = 1$ in (42), as follows

$$F_{\gamma_{FSO}}^{G\text{-}G}(\gamma) = \mathcal{K} G_{s+1,3s+1}^{3s,1} \left[\mathcal{L} \frac{\gamma}{\mu_s} \bigg|_{\mathbf{x}_3,\,0}^{1,\,\mathbf{x}_1} \right], \tag{45}$$

where $\mathcal{K} = \zeta^2 s^{\alpha+\beta-1} / [(4\pi)^{s-1} \Gamma(\alpha)\Gamma(\beta)]$, $\mathcal{L} = w(\zeta^2 \alpha\beta)^s / [(\zeta^2+1)s^2]^s$, and $\mathbf{x}_3 = \frac{\zeta^2}{s}, \dots \frac{\zeta^2+s-1}{s}, \frac{\alpha}{s}, \dots \frac{\alpha+s-1}{s}, \frac{\beta}{s}, \dots \frac{\beta+s-1}{s}$ includes $3s$ terms.

3.4 Asymptotic Bit Error Rate

The derived average BER in (44) is complicated, and hence it is hard to analyze how this BER is influenced by our system parameters. Therefore, to have more insight about the effects of our system parameters on its BER, let us drive the asymptotic average BER (P_{BER}^a) in the high SNR regime. To do that, we begin by omitting the last term in (38) because it is negligible at the high SNRs. Then, we modify the rest of (38) to get the asymptotic average BER as follows

$$P_{BER}^a = P_{BER}^{a^{hp1}} + P_{BER}^{a^{hp2}}, \tag{46}$$

where $P_{BER}^{a^{hp1}}$ and $P_{BER}^{a^{hp2}}$ are, respectively, the asymptotic average BERs for the first and second hops in the high SNR regime. Next, to obtain $P_{BER}^{a^{hp1}}$ we solve the integration in (39), but after replacing

$F_{\gamma_{RF}}(\gamma)$ with $F_{\gamma_{RF}}^{(a)}(\gamma)$ from (23) and with the help of [32, Eq. (3.381.4)], to get

$$P_{BER}^{a^{hp1}} = \frac{a_1 \, \Gamma \, (k+0.5)}{2\sqrt{\pi} \, k! \, b_1^k} \left(\frac{k}{\bar{\gamma}_{RF}}\right)^k. \tag{47}$$

On the other hand, $P_{BER}^{a^{hp2}}$ can be derived from (43) by using [38, Eq.(07.34.06.0006.01)], and mimicking the same method which is followed in deriving $F_{\gamma_{FSO}^{eff}}^{\mathcal{M}(a)}(\gamma)$ (Eqs. (24) and (25)), to get

$$P_{BER}^{a^{hp2}} = \frac{a_2 D}{2\sqrt{\pi}} \sum_{m=1}^{\beta} c_m \frac{\Gamma\left(b_{min}'/s+0.5\right) \prod_{j=1, sx_{2j} \neq b_{min}'}^{3s} \Gamma\left(x_{2j}-b_{min}'/s\right)}{(b_{min}'/s) \prod_{j=1}^{s} \Gamma(x_{1j}-b_{min}'/s)} \left(\frac{E}{b_2 \, \mu_s}\right)^{b_{min}'/s}. \tag{48}$$

For the case of $\rho \neq 1$, and by utilizing the definition of b_{min}', (48) can be compactly expressed as

$$P_{BER}^{a^{hp2}} = \frac{a_2 \, D \, \Gamma\left(b_{min}''/s+0.5\right) J}{2\sqrt{\pi} \, (b_{min}''/s) \prod_{j=1}^{s} \Gamma(x_{1j}-b_{min}''/s)} \left(\frac{E}{b_2 \, \mu_s}\right)^{b_{min}''/s}, \tag{49}$$

where x_{1j} is the jth term in $\mathbf{x}_1$,

$$J \triangleq \begin{cases} \sum_{m=1}^{\beta} c_m \prod_{j=1, sx_{2j} \neq b_{min}'}^{3s} \Gamma\left(x_{2j}-b_{min}'/s\right) & \text{if} \quad \xi^2 \text{ or } \alpha < 1, \Rightarrow b_{min}' = \min[\xi^2, \alpha] \\ \sum_{m=1}^{1} c_m \prod_{j=1, sx_{2j} \neq 1}^{3s} \Gamma\left(x_{2j}-1/s\right) & \text{if} \quad \xi^2 \, \& \alpha > 1, \Rightarrow b_{min}' = 1 \end{cases}, \tag{50}$$

and x_{2j} is the jth term in $\mathbf{x}_2$.

Thus, by substituting (47) and (49) in (46), we attain

$$P_{BER}^{a} = \frac{a_1 \, \Gamma \, (k+0.5)}{2\sqrt{\pi} \, k! \, b_1^k} \left(\frac{\bar{\gamma}_{RF}}{k}\right)^{-k} + \frac{a_2 \, D \, \Gamma\left(b_{min}''/s+0.5\right) J}{2\sqrt{\pi} \, (b_{min}''/s) \prod_{j=1}^{s} \Gamma(x_{1j}-b_{min}''/s)} \left(\frac{b_2 \, \mu_s}{E}\right)^{-b_{min}''/s}. \tag{51}$$

Of course, the $P_{BER}^{a^{hp2}}$ in (49), and accordingly the P_{BER}^{a} in (51), is when the FSO link meets $\mathcal{M}$ fading with $\rho \neq 1$. However, by setting $\rho = 1$, and for normalization $\Omega' = 1$, in (48), we can get the $P_{BER}^{a^{hp2}}$, and its correspondent P_{BER}^{a}, for the special case of G-G faded FSO link as

$$P_{BER}^{a^{hp2}} = \frac{a_2 \mathcal{K}}{2\sqrt{\pi}} \frac{\Gamma\left(b_{min}^{\star}/s+0.5\right) \prod_{j=1, sx_{3j} \neq b_{min}^{\star}}^{3s} \Gamma\left(x_{3j}-b_{min}^{\star}/s\right)}{(b_{min}^{\star}/s) \prod_{j=1}^{s} \Gamma(x_{1j}-b_{min}^{\star}/s)} \left(\frac{\mathcal{L}}{b_2 \, \mu_s}\right)^{b_{min}^{\star}/s}, \tag{52}$$

$$P_{BER}^{a} = \frac{a_1 \, \Gamma \, (k+0.5)}{2\sqrt{\pi} \, k! \, b_1^k} \left(\frac{\bar{\gamma}_{RF}}{k}\right)^{-k} + \frac{a_2 \mathcal{K}}{2\sqrt{\pi}} \frac{\Gamma\left(b_{min}^{\star}/s+0.5\right) \prod_{j=1, sx_{3j} \neq b_{min}^{\star}}^{3s} \Gamma\left(x_{3j}-b_{min}^{\star}/s\right)}{(b_{min}^{\star}/s) \prod_{j=1}^{s} \Gamma(x_{1j}-b_{min}^{\star}/s)} \left(\frac{b_2 \, \mu_s}{\mathcal{L}}\right)^{-b_{min}^{\star}/s}. \tag{53}$$

In fact as the $P_{out}^{(a)}$, in the high SNR regime, the asymptotic average BER can be typically given as $P_{BER}^{a} \simeq (\mathcal{G}_c \text{SNR})^{-\mathcal{G}_d}$, where $\mathcal{G}_d$ and $\mathcal{G}_c$ are BER performance indicators which, respectively, designate the diversity order and the coding gain related to the BER of the system[41]. Therefore, from Eqs. (51) and (53), and by keeping the standard P_{BER}^{a} in mind, it can be noticed that our system has BER-based diversity orders ($\mathcal{G}_d^{RF}$, $\mathcal{G}_d^{\mathcal{M}}$, $\mathcal{G}_d^{G-G}$) which, respectively, equal its P_{out}-based diversity orders (G_d^{RF}, $G_d^{\mathcal{M}}$, G_d^{G-G}) in each one of the previous analyzed cases in Section 3-B. However, this is not the case for the coding gains (i.e., $\mathcal{G}_c^{RF}$, $\mathcal{G}_c^{\mathcal{M}}$, $\mathcal{G}_c^{G-G}$ are, respectively, not equal to G_c^{RF}, $G_c^{\mathcal{M}}$, G_c^{G-G})[14].

Also, from (51) and (53), we can perceive that the used modulation type affects only the $\mathcal{G}_c$, while the encountered fading model (Nakagami-m, $\mathcal{M}$, G-G) affects both the $\mathcal{G}_d$ and $\mathcal{G}_c$.

---

[14]This diversity-coding gains analysis, for both P_{out} and P_{BER}, has not been done in the open literature as per our knowledge. Recently a related diversity-coding gains analysis was done in [37]. However, the outcomes drawn from that analysis are different from our $\mathcal{G}_d^{\mathcal{M}}, \mathcal{G}_c^{\mathcal{M}}, \mathcal{G}_c^{G-G}, G_d^{\mathcal{M}}, G_c^{\mathcal{M}}$, and G_c^{G-G} which are obtained here from the detailed diversity-coding gains derivations given in ((22)–(32), (46)–(53)).

3.5 Ergodic Channel Capacity

Ergodic channel capacity (C_{erg}) is the term used for information theoretical channel capacity in case of fast fading channels [35]. As a dual hop DF system, our system[15] has the following ergodic capacity

$$C_{\text{erg}} = \frac{1}{2} \min \left[\mathbb{E}\{C_{\text{RF}}\}, \mathbb{E}\{C_{\text{FSO}}\} \right], \tag{54}$$

where C_{RF} and C_{FSO} are defined in (11) and (13), respectively, and thus the above expectations are given by

$$\mathbb{E}\{C_{\text{RF}}\} = \frac{1}{\ln(2)} \int_0^\infty \ln(1 + \gamma) f_{\gamma_{\text{RF}}}(\gamma) \, d\gamma. \tag{55}$$

$$\mathbb{E}\{C_{\text{FSO}}\} = \frac{1}{\ln(2)} \int_0^\infty \ln(1 + \gamma) f_{\gamma_{\text{FSO}}^{\text{eff}}}^{\mathcal{M}}(\gamma) \, d\gamma. \tag{56}$$

Now upon substituting (2) in (55), while utilizing $\ln(1+\gamma) = G_{2,2}^{1,2}\left[\gamma \Big|_{1,0}^{1,1}\right]$ and $\exp(-z) = G_{0,1}^{1,0}\left[z \Big|_{0}^{-}\right]$, and with the help of [38, Eq. (07.34.21.0013.01), Eq. (07.34.17.0011.01)], we get

$$\mathbb{E}\{C_{\text{RF}}\} = \frac{1}{(k-1)! \ln 2} G_{2,3}^{3,1}\left[\frac{k}{\bar{\gamma}_{\text{RF}}} \Big|_{k,0,0}^{0,1}\right]. \tag{57}$$

Then again, after substituting (14) in (56) and utilizing $\ln(1+\gamma) = G_{2,2}^{1,2}\left[\gamma \Big|_{1,0}^{1,1}\right]$, $\mathbb{E}\{C_{\text{FSO}}\}$ can be attained by using [38, Eq. (07.34.21.0013.01)]. By doing that, and making some simplifications by exploiting the Meijer's G-function definition [32, Eq. (9.301)], we obtain

$$\mathbb{E}\{C_{\text{FSO}}\} = \frac{\xi^2 A/2}{(2\pi)^{w-1} \ln 2} \sum_{m=1}^{\beta} b_m G_{w+2,w+4}^{w+4,w}\left[\frac{B/c^w}{\mu_s^{1/s}} \Bigg|_{\xi^2,\,\alpha,\,m,\,0,\,\mathbf{x}_4}^{\mathbf{x}_4,\,1,\,\xi^2+1}\right], \tag{58}$$

where $\mathbf{x}_4 = \frac{0}{w}, \cdots, \frac{w-1}{w}$ includes w terms.

Finally, by substituting (57) and (58) in (54), we get our system Ergodic capacity.

Recall that the $\mathbb{E}\{C_{\text{FSO}}\}$ in (58) is for the $\mathcal{M}$ faded FSO link. Instead, to obtain the $\mathbb{E}\{C_{\text{FSO}}\}$ for the special case of G-G faded FSO link, the pdf $f_{\gamma_{\text{FSO}}^{\text{eff}}}^{\mathcal{M}}(\gamma)$ in (56) should be replaced by the pdf $f_{\gamma_{\text{FSO}}^{\text{eff}}}^{\text{G-G}}(\gamma)$ given in (15). Doing that, and following the same previous steps, results in

$$\mathbb{E}\{C_{\text{FSO}}\} = \frac{\xi^2/(\Gamma(\alpha)\Gamma(\beta))}{(2\pi)^{w-1} \ln 2} G_{w+2,w+4}^{w+4,w}\left[\frac{\xi^2 \alpha\beta/c^w}{(\xi^2+1)\mu_s^{1/s}} \Bigg|_{\xi^2,\,\alpha,\,\beta,\,0,\,\mathbf{x}_4}^{\mathbf{x}_4,\,1,\,\xi^2+1}\right]. \tag{59}$$

4. Simulation and Numerical Results

In this section, we present numerical examples to illustrate the analytical and asymptotic expressions of the previous section and also to show the effect of the different fading parameters and pointing error on the system performance.[16] Additionally, this section validates the derived analytical and asymptotic expressions by Monte-Carlo simulations. In these simulations, 10^6 realizations of the SNR random variable are used except at the results which are less than 10^{-6} where 10^8 realizations are used. Also, BPSK ($a_1 = b_1 = 1$) and OOK ($a_2 = 1, b_2 = 0.5$) are used in the results of the BER as the modulation schemes for the RF and IMDD-FSO hops, respectively, while BPSK ($a_2 = b_2 = 1$) is used for HD-FSO hop.

---

[15]In general, the RF and FSO faded channels are a slow fading channels. However, they can be considered as fast fading channels, if long enough interleaving is used. This interleaving-based fast fading consideration can be especially valid in some situations such as in windy conditions where RF and FSO channels (particularly FSO pointing errors) fluctuate relatively fast.

[16]Following the same strategy as in related literature, see e.g. [15], [18], [29], [30], [37], we chose the values of the system parameters to validate the derived expressions, and thus other parameters' values can be used by planning engineers to get the results in their particular scenarios.
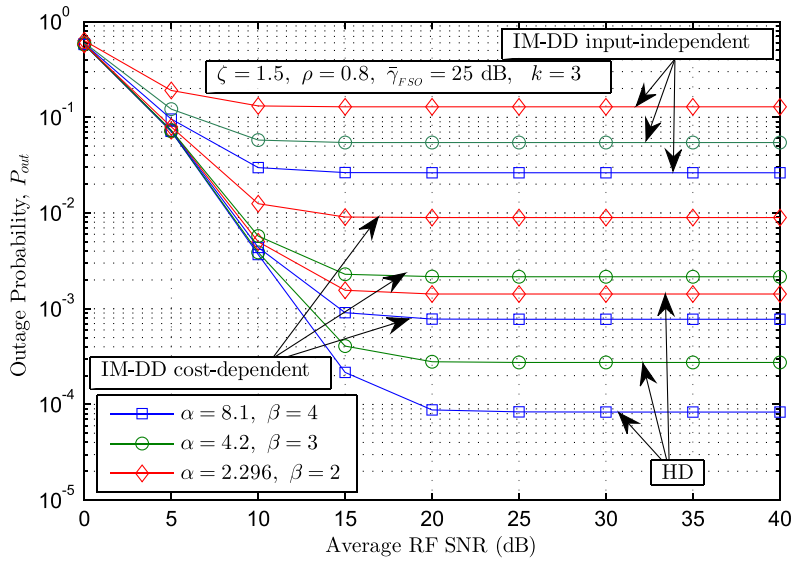
Fig. 2. P_{out} for different values of α and β considering all FSO detection techniques.
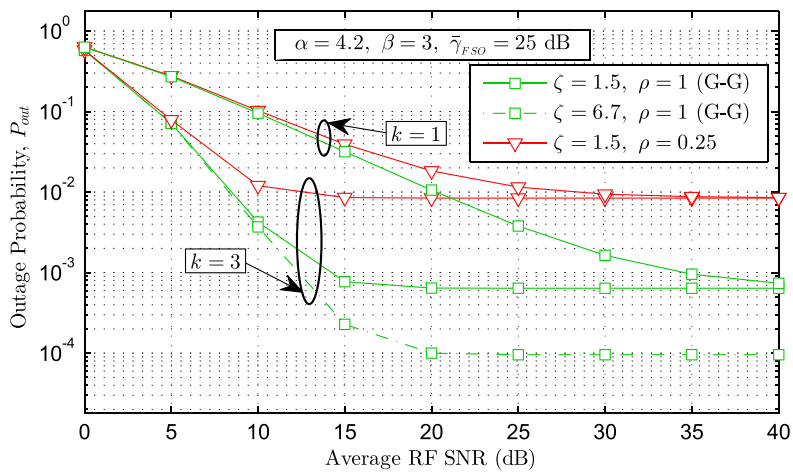

Fig. 3. P_{out} for different values of k, ρ and ζ considering IM-DD cost-dependent FSO link.

Fig. 2 demonstrates the effect of the atmospheric turbulence parameters (α and β) on our system P_{out} for a specific pointing error ($\zeta = 1.5$).[17] From this figure, it can be noticed that the lower values of α and β, i.e., stronger atmospheric turbulence, result in higher (worse) P_{out} and vice versa.[18]

The effect of different values of k, ρ, and ζ(pointing error) on our system outage probability (P_{out}) is demonstrated in Fig. 3 for fixed atmospheric turbulence conditions considering IM-DD cost-dependent. As can be seen, the higher the values of k, ρ, or ζ(smaller pointing errors), the lower is P_{out}, and hence the better is the attained performance. Also, based on the used parameters, we can perceive from Fig. 2 and Fig. 3 that in the low RF SNRs, the RF hop dominates P_{out}, i.e., P_{out} varies when $\bar{\gamma}_{RF}$ changes although $\bar{\gamma}_{FSO}$ is constant here. However, in these figures when the RF

---

[17]In all results, without loss of generality, we use $\gamma_{out} = 0$ dB, $\Omega = 0.78$, and $b_0 = 0.11$.

[18]Note that $\bar{\gamma}_{HD}$ and $\bar{\gamma}_{IMDD_{cost}}$ are proportional to P_r, whereas $\bar{\gamma}_{IMDD_{indp}}$ is proportional to P_r^2. Therefore the results plotted versus the average SNR should not be used in comparing the different FSO detectors, otherwise this will lead to unfair comparison from P_r point of view.
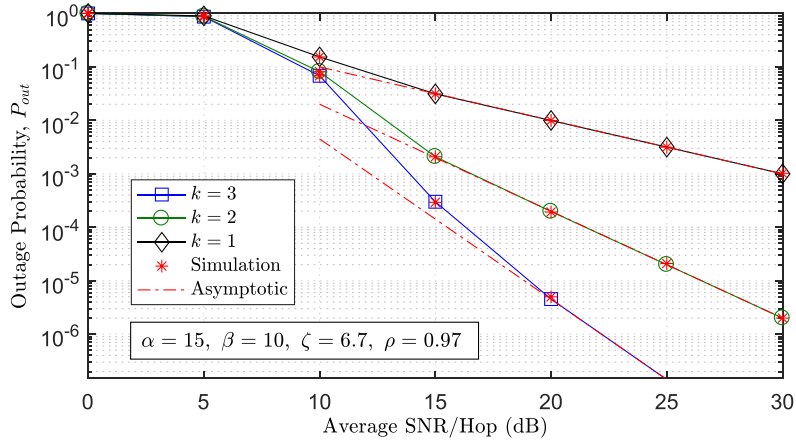
Fig. 4. P_{out} dominated by the RF hop when IM-DD cost-dependent is used in the FSO hop.
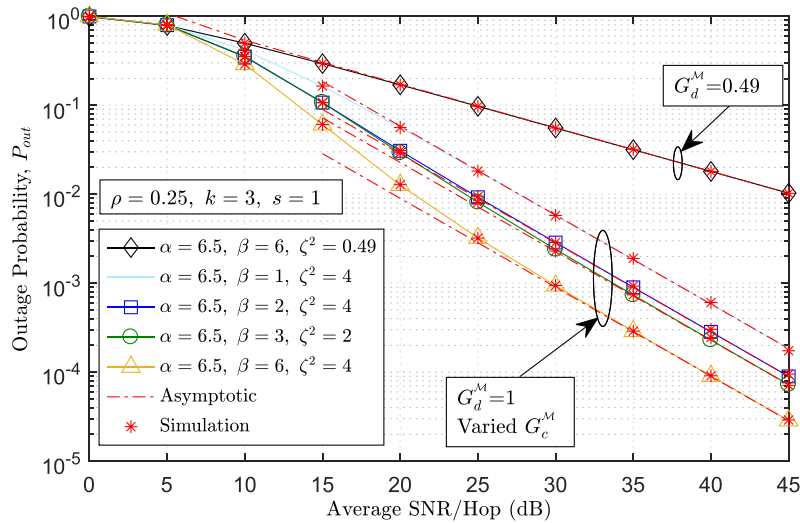

Fig. 5. P_{out} dominated by IM-DD cost-dependent FSO hop.

SNR becomes relatively high, the P_{out} becomes constant because in this case it is dominated by the FSO hop whose $\bar{\gamma}_{FSO}$ is set constant in these figures.

Figs. 4, 5, and 6 evince that the asymptotic P_{out} expression converges to the exact P_{out} expression at the high SNRs. Additionally, these figures show the coding gain and diversity order of our system outage probability at high SNRs in different cases. More specifically, Fig. 4 confirms that $G_d^{RF} = k$ as derived in case 1 of Section 3-B, i.e., the measured slopes of the log-log curves in the high SNR from Fig. 4 equal the derived G_d^{RF}.

On the other hand, Fig. 5 confirms that, given $s = 1$, $G_d^{\mathcal{M}} = b_{min}^{''}/s = \min[\zeta^2, \alpha, 1]$ as derived in (29a). To explain this, we labeled two groups in this figure. In the group of $G_d^{\mathcal{M}} = 1$, the values of β, ζ are changed among this group curves but they still have $\min[\zeta^2, \alpha, 1] = 1 \Rightarrow G_d^{\mathcal{M}} = 1$ which is identical to their log-log slope in the figure. Whereas, the difference in β, ζ among this group produces different $G_c^{\mathcal{M}}$ in each of its curves. The other group has $\min[\zeta^2, \alpha, 1] = \zeta^2 \Rightarrow G_d^{\mathcal{M}} = 0.49$ which is identical to its log-log slope. Alternatively, Fig. 6 proves that, given $s = 1$, $G_d^{G-G} = b_{min}^{\star}/s = \min[\zeta^2, \alpha, \beta]$ as derived previously, i.e., the labeled measured log-log slopes from Fig. 6 are identical to the derived G_d^{G-G} in (33b).
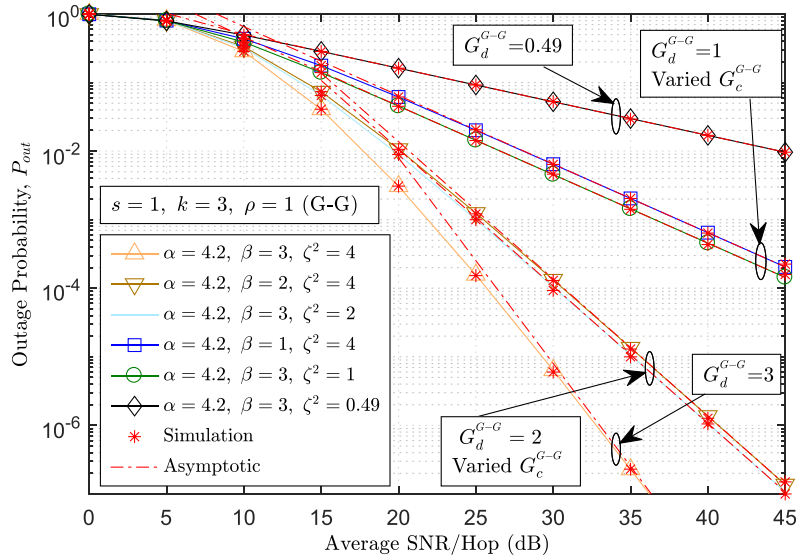
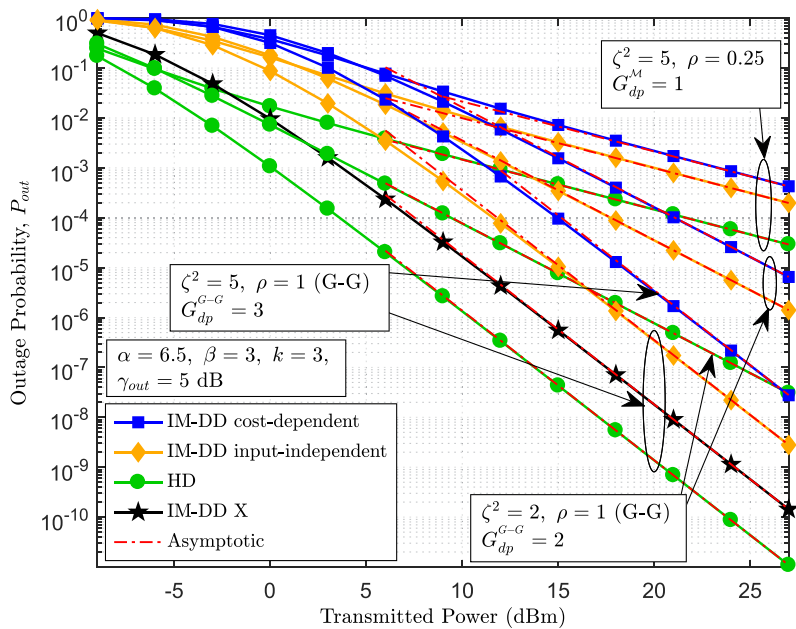Fig. 6. P_{out} dominated by IM-DD cost-dependent G-G FSO hop.

Fig. 7. P_{out} dominated by the FSO hop vs transmitted power.

Moreover, Figs. 4, 5, and 6 confirm the validity of the derived analytical and asymptotic P_{out} expressions by showing the perfect match between them and the Monte-Carlo simulations.

Fig. 7 shows that the asymptotic P_{out} expression converges to the exact P_{out} at the high transmitted powers. Also, this figure validates that, at high transmitted powers, all FSO detectors result in the same diversity order which is given by $G_{dp}^{\mathcal{M}} = \min[\zeta^2, \alpha, 1]$ or $G_{dp}^{\text{G-G}} = \min[\zeta^2, \alpha, \beta]$ as deduced in (34), i.e., in Fig. 7 the labeled measured log-log slopes are the same as the earlier deduced ones. Additionally, from this figure, due to the different coding gains, we can see that the HD offers better outage performance than both IM-DD techniques, and IM-DD input-independent reveals less P_{out} than IM-DD cost-dependent. However, based on the used parameters in Fig. 7, this IM-DD
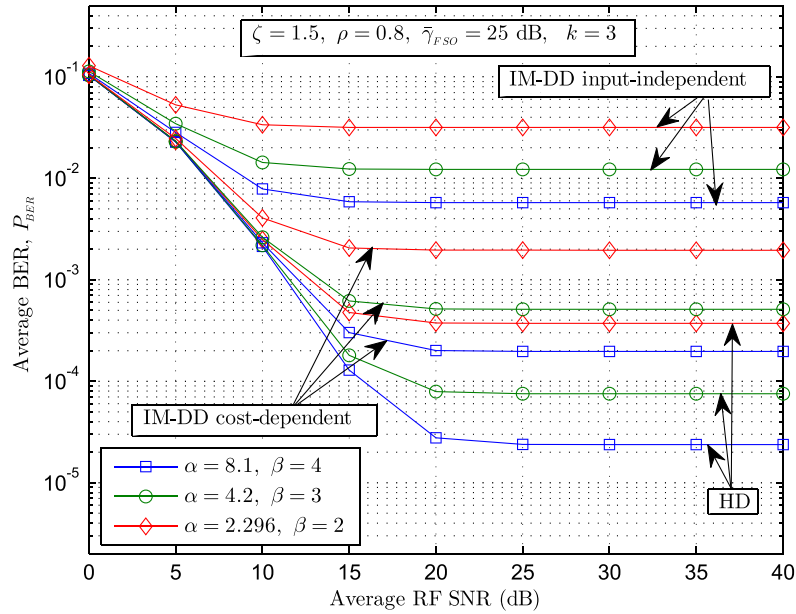
Fig. 8. P_{BER} for different values of α and β considering all FSO detection techniques.

input-independent outage is overestimated because the IM-DD input-independent ignores the shot-noise which is considerable in this example.

For comparison, Fig. 7 also includes a curve labeled *IM-DD X*. This curve reflects the overestimation (misconception) in the outage probability P_{out} when we unsoundly use Shannon's capacity $\left(\log\left(1 + \gamma_{\text{IMDD}_{indp}}\right)\right)$ for IM-DD input-independent, see e.g., [14], [17], [18], [37], instead of its precise capacity approx. $\left(\log\left(1 + \sqrt{\frac{e}{2\pi}\gamma_{\text{IMDD}_{indp}}}\right)\right)$ which is used here in our work. Specifically, as deduced in Section 3-B, Fig. 7 proves that, under the same parameters, IM-DD X holds the same G_d as all FSO detectors, including IM-DD input-independent. Alternatively, this figure evinces that, under the same parameters, there is an overestimation in G_c reflected by IM-DD X as compared to the precise IM-DD input-independent curve. It can be seen that, given $\gamma_{out} = 5$ dB, this overestimation is consistent with the drawn one in (37) (i.e., $\delta G_{cp} = 5\log_{10}(\gamma_{out}) + 1.819 = 4.319$ dB).

Alternatively, Fig. 8 illustrates the influence of the atmospheric turbulence parameters (α and β) on our system P_{BER} for a fixed pointing error ($\zeta = 1.5$). From this figure, it can be observed that higher values of α and β, i.e., weaker atmospheric turbulence, result in a lower (better) P_{BER} and vice versa. Another note, based on the used parameters, in Fig. 8 is that in the relatively high RF SNR regime, the P_{BER} is constant, since in this regime it is dominated by the FSO hop whose $\bar{\gamma}_{\text{FSO}}$ is kept constant in this figure, however in the low RF SNRs the P_{BER} is dominated by the RF hop.

The impact of the different values of ρ, k, and ζ on the BER (P_{BER}) is shown in Fig. 9 for IM-DD cost-dependent. As can be seen, an increase in the value of ρ, k, or ζ (smaller pointing errors) leads to a decrease in the P_{BER}, and hence results in a better performance. Beside that, Fig. 9 reveals the convergence between the asymptotic and exact P_{BER} expressions. Furthermore, Fig. 9 validates that, given $s = 1$, $\mathcal{G}_d^{\mathcal{M}} = b''_{\min}/s = \min[\zeta^2, \alpha, 1]$ and $\mathcal{G}_d^{\text{G-G}} = b^\star_{\min}/s = \min[\zeta^2, \alpha, \beta]$ as drawn in Section 3-D, i.e., in Fig. 9 the labeled measured log-log slopes are identical to the formerly drawn ones.

The ergodic channel capacity (C_{erg}) versus the RF SNR ($\bar{\gamma}_{\text{RF}}$) is shown in Fig. 10 for various values of the turbulence parameters (α and β), while the FSO SNR ($\bar{\gamma}_{\text{FSO}}$) and the pointing error (ζ) are kept fixed in this figure. It can be seen, from this figure, that lower values of α and β, i.e., stronger atmospheric turbulence, result in lower (worse) C_{erg} and vice versa. Moreover, based on the used parameters, we can notice from Fig. 10 that in the relatively low RF SNRs the RF hop dominates the C_{erg}, i.e., C_{erg} varies with the change in $\bar{\gamma}_{\text{RF}}$ although $\bar{\gamma}_{\text{FSO}}$ is set constant here. However, if the
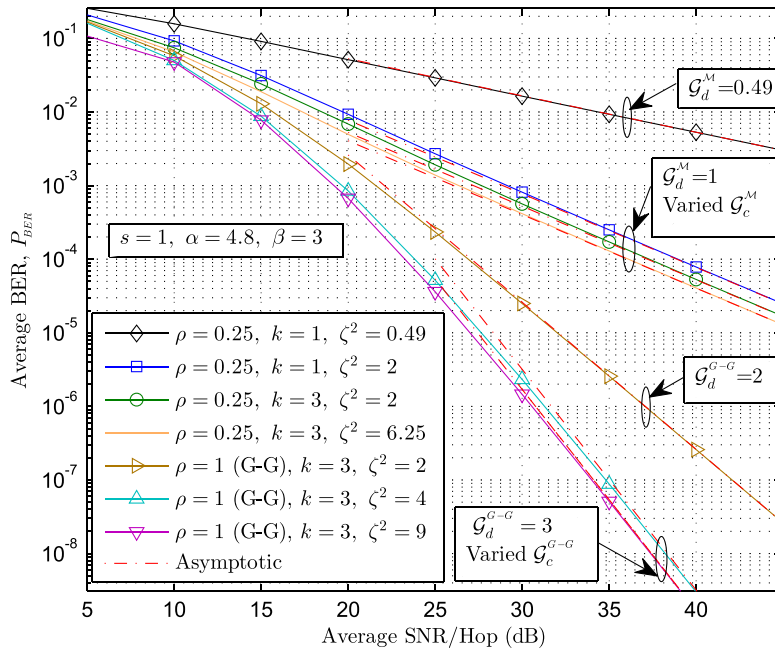
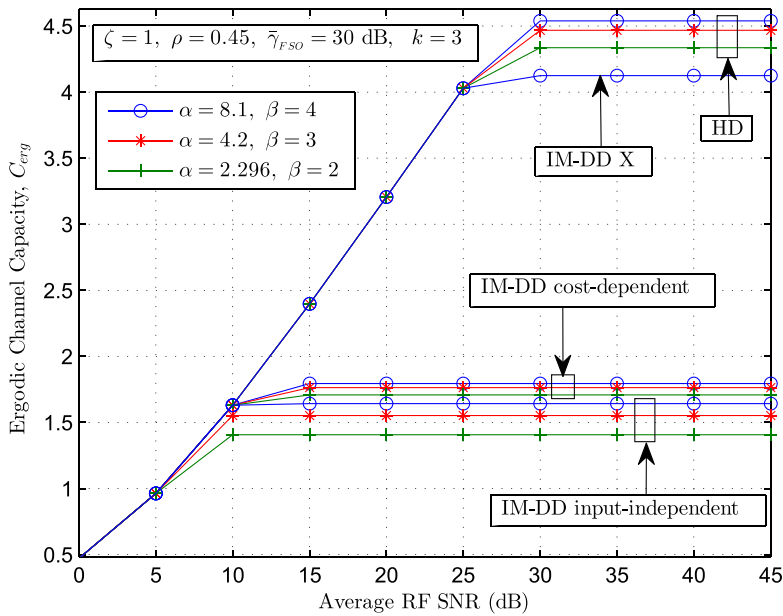Fig. 9. P_{BER} dominated by IM-DD cost-dependent FSO hop for different values of k, ρ and ζ.

Fig. 10. C_{erg} for different values of α and β considering all FSO detection techniques.

RF SNR becomes relatively high, C_{erg} will be constant, because in this case it will be dominated by the FSO hop whose $\bar{\gamma}_{\text{FSO}}$ is set constant in this figure.

Fig. 11 provides the influence of the different values of ρ and ζ on the system ergodic channel capacity (C_{erg}) for all FSO detectors. Clearly, C_{erg} increases by the increase in the value of ρ or ζ(smaller pointing error). In addition, this figure demonstrates that the HD provides better ergodic capacity than both IM-DD techniques, and IM-DD input-independent reveals higher C_{erg} than IM-DD cost-dependent. However, based on the used parameters in this figure, this IM-DD
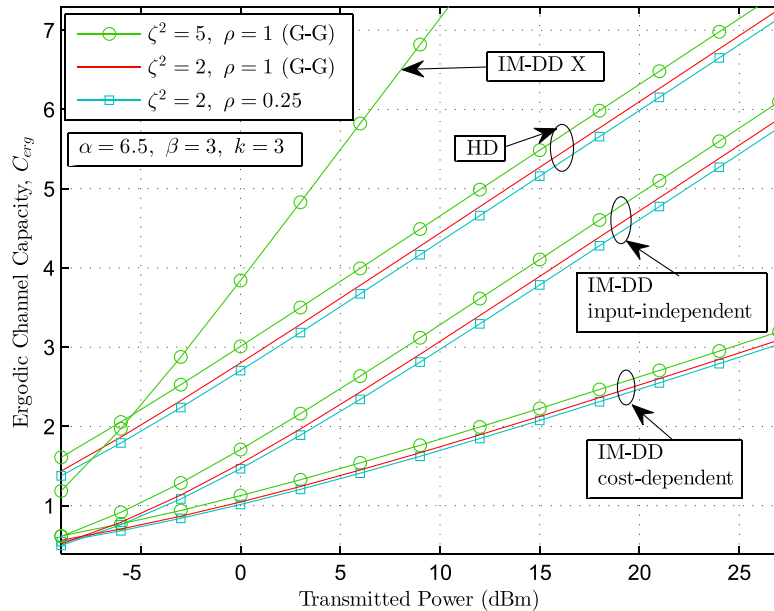
Fig. 11. C_{erg} dominated by the FSO hop vs transmitted power.

input-independent ergodic capacity is overestimated because again the IM-DD input-independent ignores the shot-noise which is considerable in this example. Furthermore, from Fig. 11 it can be seen that the capacity pre-log equals 0.5 for HD and IM-DD input-independent, while it is 0.25 for IM-DD cost-dependent. This confirms the capacity pre-log, assuming Tx over 2 channel uses, that can be deduced, at high transmitted powers, from $\mathbb{E}\{C_{\text{FSO}}\}$ with the help of (13), (12) and (5).

Then again for comparison, Figs. 10 and 11 contain the curve IM-DD X which reveals the overestimation in C_{erg} if the capacity form IM-DD_capX $\left(\log\left(1 + \gamma_{\text{IMDD}_{indp}}\right)\right)$ is unsoundly used for IM-DD input-independent instead of its precise capacity approx. $\left(\log\left(1 + \sqrt{\frac{e}{2\pi}\gamma_{\text{IMDD}_{indp}}}\right)\right)$ given in (12). This overestimation, in C_{erg} (and its pre-log) of IM-DD input-independent, is mainly due to the missed sqrt. in the IM-DD_capX form as compared to the one in (12), i.e., even if a form such as $\left(\log\left(1 + \frac{e}{2\pi}\gamma_{\text{IMDD}_{indp}}\right)\right)$ is inaccurately used for IM-DD input-independent capacity, the same above indicated overestimation, in the pre-log of C_{erg}, will appear.

5. Conclusion

In this work, we studied the performance of dual-hop mixed RF/ FSO DF relaying, where HD and IM-DD were considered in a unified manner for FSO detection. Specifically, we derived closed-form expressions for the outage probability, average BER, and ergodic capacity of this system assuming generalized fading models, i.e., Nakagami-m and $\mathcal{M}$ fading with pointing error for the RF and FSO channels, respectively. In doing that, we utilized, for the first time as per our knowledge, a precise IM-DD channel capacity result. Moreover, this was the first time that not only the IM-DD input-independent but also the IM-DD cost-dependent AWGN channel is considered in such system analysis. Also, in BER analysis, we assumed that the modulation schemes in the two hops can be different, as not all modulations are suitable for FSO IM-DD links. Additionally, the system performance was asymptotically investigated at high SNR where new non-reported diversity order and coding gain analyses was shown. Interestingly, we found that in the FSO hop, at high transmitted powers, all the optical detectors result in the same diversity order, whereas their coding gains are different. Also, for HD and IM-DD input-independent we found that, at high transmitted powers, their capacities pre-logs are identical and equal twice the one of IM-DD cost-dependent.

Moreover, we showed the overestimations which occur in the outage and capacity of the system when the well-known Shannon's AWGN channel capacity is used for IM-DD instead of its precise capacity approx. These overestimations lead to misconception in the comparison between HD and IM-DD. Furthermore, we offered simulation results that confirm the derived exact and asymptotic expressions.

References

[1] O. M. S. Al-Ebraheemy, A. M. Salhab, A. Chaaban, S. A. Zummo, and M.-S. Alouini, "Precise outage analysis of mixed RF/unified-FSO DF relaying with HD and 2 IM-DD channel models," in *Proc. 13th Int. Wireless Commun. Mobile Comput. Conf.*, Valencia, Spain, Jun. 2017, pp. 1184–1189.

[2] S. Arnon, J. Barry, G. Karagiannidis, R. Schober, and M. Uysal, *Advanced Optical Wireless Communication Systems*. Cambridge, U.K.: Cambridge Univ. Press, 2012.

[3] M. A. Khalighi and M. Uysal, "Survey on free space optical communications: A communication theory perspective," *IEEE Commun. Surveys Tut.*, vol. 16, no. 4, pp. 2231–2258, Fourth Quarter 2014.

[4] M. Karimi and M. Nasiri-Kenari *et al.*, "Outage analysis of relay-assisted free-space optical," *IET Commun.*, vol. 4, no. 12, pp. 1423–1432, 2010. doi: 10.1049/iet-com.2009.0335.

[5] M. A. Kashani, M. M. Rad, M. Safari, and M. Uysal, "All-optical amplify-and-forward relaying system for atmospheric channels," *IEEE Commun. Lett.*, vol. 16, no. 10, pp. 1684–1687, Oct. 2012.

[6] M. R. Bhatnagar, "Performance analysis of decode-and-forward relaying in Gamma-Gamma fading Channels," *IEEE Photon. Technol. Lett.*, vol. 24, no. 7, pp. 545–547, Apr. 2012.

[7] P. Puri, P. Garg, and M. Aggarwal, "Outage and error rate analysis of network-coded coherent TWR-FSO systems," *IEEE Photon. Technol. Lett.*, vol. 26, no. 18, pp. 1797–1800, Sep. 2014.

[8] I. S. Ansari, F. Yilmaz, and M.-S. Alouini, "On the performance of mixed RF/FSO variable gain dual-hop transmission systems with pointing errors," in *Proc. IEEE Veh. Tech. Conf.*, Sep. 2–5, 2013, pp. 1–5.

[9] M. R. Bhatnagar and M. K. Arti, "Performance analysis of hybrid satellite-terrestrial FSO cooperative system," *IEEE Photon. Technol. Lett.*, vol. 25, no. 22, pp. 2197–2200, Nov. 2013.

[10] I. S. Ansari, F. Yilmaz, and M.-S. Alouini, "Impact of pointing errors on the performance of mixed RF/FSO dual-hop transmission systems," *IEEE Wireless Commun. Lett.*, vol. 2, no. 3, pp. 351–354, Jun. 2013.

[11] I. S. Ansari, M.-S. Alouini, and F. Yilmaz, "On the performance of hybrid RF and RF/FSO fixed gain dual-hop transmission systems," in *Proc. Saudi Int. Electron., Commun. Photon. Conf.*, Riyadh, Saudi Arabia, Apr. 27–30, 2013, pp. 1–6.

[12] S. Anees and M. Bhatnagar, "Performance of an amplify-and-forward dual-hop asymmetric RF/FSO communication system," *IEEE/OSA J. Opt. Commun. Netw.*, vol. 7, no. 2, pp. 124–135, Feb. 2015.

[13] E. Zedini, I. Ansari, and M.-S. Alouini, "On the performance of hybrid line of sight RF and RF-FSO fixed gain dual-hop transmission systems," in *Proc. IEEE Global Commun. Conf.*, Dec. 2014, pp. 2119–2124.

[14] E. Zedini, I. S. Ansari, and M.-S. Alouini, "Performance analysis of mixed Nakagami-*m* and Gamma-Gamma dual-hop FSO transmission systems," *IEEE Photon. J.*, vol. 7, no. 1, Feb. 2015, Art. no. 7900120.

[15] A. M. Salhab, F. S. Al-Qahtani, R. M. Radaydeh, S. A. Zummo, and H. Alnuweiri, "Power allocation and performance of multiuser mixed RF/FSO relay networks with opportunistic scheduling and outdated channel information," *IEEE/OSA J. Lightw. Technol.*, vol. 34, no. 13, pp. 3259–3272, Jul. 2016.

[16] E. S.-Nasab and M. Uysal, "Generalized performance analysis of mixed RF/FSO cooperative systems," *IEEE Trans. Wireless Commun.*, vol. 15, no. 1, pp. 714–727, Jan. 2016.

[17] S. Anees and M. R. Bhatnagar, "Performance evaluation of decode-and-forward dualhop asymmetric RF-FSO system," *IET Optoelect.*, vol. 9, no. 5, pp. 232–240, 2015.

[18] N. I. Miridakis, M. Matthaiou, and G. K. Karagiannidis, "Multiuser relaying over mixed RF/FSO links," *IEEE Trans. Commun.*, vol. 62, no. 5, pp. 1634–1645, May 2014.

[19] S. Anees and M. R. Bhatnagar, "Exact performance analysis of DF based mixed triple-hop RF/FSO/RF communication system," in *Proc. IEEE 28th Int. Symp. Personal, Indoor, Mobile Radio Commun.*, 2017, pp. 1–5.

[20] S. Anees, P. S. S. Harsha, and M. R. Bhatnagar, "On the performance of AF based mixed triple-hop RF/FSO/RF communication system," in *Proc. IEEE 28th Int. Symp. Personal, Indoor, Mobile Radio Commun.*, 2017, pp. 1–6.

[21] A. M. Salhab, "A new scenario of triple-hop mixed RF/FSO/RF relay network with generalized order user scheduling and power allocation," *EURASIP J. Wireless Commun. Netw.*, vol. 2016, no. 1, Dec. 2016.

[22] C. E. Shannon, "A mathematical theory of communication," *Bell Syst. Tech. J.*, vol. 27, pp. 379–423, 623–656, 1948.

[23] A. Lapidoth, S. M. Moser, and M. Wigger, "On the capacity of free-space optical intensity channels," *IEEE Trans. Inf. Theory*, vol. 55, no. 10, pp. 4449–4461, Oct. 2009.

[24] A. Farid and S. Hranilovic, "Capacity bounds for wireless optical intensity channels with gaussian noise," *IEEE Trans. Inf. Theory*, vol. 56, no. 12, pp. 6066–6077, Dec. 2010.

[25] A. Chaaban, J. M. Morvan, and M.-S. Alouini, "Free-space optical communications: Capacity bounds, approximations, and a new sphere-packing perspective," *IEEE Trans. Commun.*, vol. 64, no. 3, pp. 1176–1191, Mar. 2016.

[26] A. Chaaban and M.-S. Alouini, "Optical intensity modulation direct detection versus heterodyne detection: A high-SNR capacity comparison," in *Proc. 5th Int. Conf. Commun. Netw.*, Tunis, Tunisia, Nov. 2015, pp. 1–5.

[27] A. Chaaban, J. M. Morvan, and M.-S. Alouini, "Free-space optical communications: Capacity bounds, approximations, and a new sphere-packing perspective," KAUST, Thuwal, Saudi Arabia, Tech. Rep., Apr. 2015. [Online]. Available: http://hdl.handle.net/10754/552096

[28] M. K. Simon and M.-S. Alouini, *Digital Communication Over Fading Channels*, 2nd ed. Hoboken, NJ, USA: Wiley, 2005.

[29] A. J. Navas, J. M. G. Balsells, J. F. Paris, and A. P. Notario, "A unifying statistical model for atmospheric optical scintillation," in *Numerical Simulations of Physical and Engineering Processes*, J. Awrejcewicz, Ed. Rijeka, Croatia: Intech, 2011, ch. 8.

[30] A. J. Navas, J. M. G. Balsells, J. F. Paris, M. C. Vazquez, and A. P. Notario, "Impact of pointing errors on the performance of generalized atmospheric optical channels," *Opt. Express*, vol. 20, no. 11, pp. 12550–12562, May 2012.

[31] A. Farid and S. Hranilovic, "Outage capacity optimization for free-space optical links with pointing errors," *IEEE/OSA J. Lightw. Technol.*, vol. 25, no. 7, pp. 1702–1710, Jul. 2007.

[32] I. S. Gradshteyn and I. M. Ryzhik, *Tables of Integrals, Series and Products*, 6th ed., San Diago, CA, USA: Acadamic, 2000.

[33] W. Gappmair, "Further results on the capacity of free-space optical channels in turbulent atmosphere," *IET Commun.*, vol. 5, no. 9, pp. 1262–1267, Jun. 2011.

[34] I. S. Ansari, F. Yilmaz, and M.-S. Alouini, "Performance analysis of FSO links over unified Gamma-Gamma turbulence channels," in *Proc. IEEE 81st Veh. Tech. Conf.*, Glasgow, Scotland, 2015, pp. 1–5.

[35] D. Tse and P. Viswanath, *Fundamentals of Wireless Communications.* Cambridge, U.K.: Cambridge Univ. Press, 2005.

[36] S. Anees and M. R. Bhatnagar, "On the capacity of decode-and-forward dual-hop free space optical communication systems," in *Proc. IEEE Wireless Commun. and Netw. Conf.*, Istanbul, Turkey, Apr. 2014, pp. 18–23.

[37] I. S. Ansari, F. Yilmaz, and M.-S. Alouini, "Performance analysis of free-space optical links over málaga ($\mathcal{M}$) turbulence channels with pointing errors," *IEEE Trans. Wireless Commun.*, vol. 15, no. 1, pp. 91–102, Jan. 2016.

[38] Wolfram, "The Wolfram functions site," 2013. [Online]. Available: http://functions.wolfram.com

[39] T. A. Tsiftsis, H. G. Sandalidis, G. K. Karagiannidis, and N. C. Sagias, "Multihop free-space optical communications over strong turbulence channels," in *Proc. IEEE Int. Conf. Commun.*, Istanbul, Turkey, Jun. 2006, pp. 2755–2759.

[40] M. R. McKay, A. L. Grant, and I. B. Collings, "Performance analysis of MIMO-MRC in double-correlated Rayleigh environments," *IEEE Trans. Commun.*, vol. 55, no. 3, pp. 497–507, Mar. 2007.

[41] J. G. Proakis, *Digital Communications*, 4th ed. New York, NY, USA: McGraw-Hill, 2001.